# DEVELOPING FRICTION STIR DIFFUSION CLADDING (FSDC) PROCESS

BY

**Almigdad Babiker Hamid Ibrahim**

A Thesis Presented to the
DEANSHIP OF GRADUATE STUDIES

**KING FAHD UNIVERSITY OF PETROLEUM & MINERALS**

DHAHRAN, SAUDI ARABIA

In Partial Fulfillment of the
Requirements for the Degree of

# MASTER OF SCIENCE

**In**

**MECHANICAL ENGINEERING**

**May 2017**

KING FAHD UNIVERSITY OF PETROLEUM & MINERALS

DHAHRAN- 31261, SAUDI ARABIA

**DEANSHIP OF GRADUATE STUDIES**

This thesis, written by **Almigdad Babiker Hamid Ibrahim** under the direction of his thesis advisor and approved by his thesis committee, has been presented and accepted by the Dean of Graduate Studies, in partial fulfillment of the requirements for the degree of **MASTER OF SCIENCE IN MECHANICAL ENGINEERING.**

Dr. Fadi Al-Badour
(Advisor)

Dr. Zuhair Mattoug Gasem
Department Chairman

Dr. Nesar Merah
(Member)

Dr. Salam A. Zummo
Dean of Graduate Studies

Dr. Tahar Laoui
(Member)

15/8/17
Date

© Almigdad Babiker Hamid Ibrahim

May 2017

***Dedication***

***To my Family, My friends and My colleagues***

***.. With Love.***

# ACKNOWLEDGMENTS

All praise is to almighty Allah for giving me the power, strength and patient to accomplish this work successfully. I would like to acknowledge King Fahd University of Petroleum and Minerals (KFUPM) for giving me this chance to pursue my Master degree.

I would like to express my appreciation to my Advisor Dr. Fadi Al-Badour for his support, guidance, friendship, comments and valuable advices during my master studies. His door was always open whenever I had any problem. Special thanks to my previous supervisor, Prof. Abdelrahman Nasr Shuaib for his guidance and support during my graduate studies at KFUPM.

I am very grateful for Dr. Rami Suleiman for his magnificent efforts and support. I would like to thank my thesis committee members, Prof. Neçar Merah and Prof Taher Laoui for their support and valuable comments on my thesis. Also, I like to thank the lab and workshop technicians who have willingly helped me during my thesis work.

I would like also to thank GARMCO Company for providing me with the raw material for my work. Also, I am very grateful for the CENT lab director Dr. Zain Yamani and Dr. Abbas Hakeem for giving me the opportunity to conduct my research work at the CENT lab.

Finally, I would like to thank my loved ones, family and my fiancé for their continuous prayers and encouragement through my master studies. I am grateful forever for your love and support.

# TABLE OF CONTENTS

**ACKNOWLEDGMENTS** ..... **V**

**TABLE OF CONTENTS** ..... **VI**

**LIST OF TABLES** ..... **IX**

**LIST OF FIGURES** ..... **IX**

**LIST OF ABBREVIATIONS** ..... **XI**

**ABSTRACT** ..... **XIII**

**ملخص الرسالة** ..... **XVI**

**CHAPTER 1 INTRODUCTION** ..... **1**

**1.1 Motivation** ..... **1**

**1.2 General Background** ..... **3**

**1.2.1 Definition of Cladding** ..... **3**

**1.2.2 Conventional cladding techniques** ..... **3**

**1.2.3 Non-conventional cladding techniques** ..... **6**

**1.2.4 Materials used in cladding process** ..... **8**

**1.3 Problem description** ..... **9**

**1.4 Friction Stir Diffusion Cladding (FSDC)** ..... **10**

**1.5 Main advantages of FSDC** ..... **14**

**1.6 Objectives** ..... **14**

**1.7 Organization** ..... **16**

**CHAPTER 2 LITERATURE REVIEW** ..... **17**

**2.1 Friction Stir Lap Welding** ..... **17**

**2.2 Friction stir processing (surface modification)** ..... **25**

2.3 Pinless FSW and Friction diffusion bonding ..... 26

2.4 Corrosion behavior of FSW joints ..... 29

CHAPTER 3 RESEARCH METHODOLOGY ..... 34

3.1 Approach ..... 34

3.2 Experimental Setup and Procedure ..... 35

3.2.1 Workpiece materials ..... 35

3.2.2 FSW machine ..... 37

3.2.3 Clamping system ..... 37

3.2.4 FSDC Tool Design ..... 39

3.2.5 Process parameters ..... 41

3.3 Characterization of cladded samples ..... 41

3.4 Corrosion Testing ..... 43

CHAPTER 4 RESULTS AND DISCUSSION ..... 46

4.1 Surface morphology ..... 46

4.1.1 The effect of process parameters on surface quality ..... 46

4.2 Microstructural and Materials characterization results ..... 51

4.2.1 Optical Microscope (OM) ..... 51

4.2.2 SEM and EDS analysis ..... 55

4.2.3 XRD results and analysis ..... 58

4.3 Mechanical tests results and discussion ..... 62

4.3.1 Microhardness ..... 62

4.3.2 Tensile-shear strength ..... 64

4.4 Corrosion (electrochemical test) results ..... 68

CHAPTER 5 CONCLUSIONS AND RECOMMENDATIONS ..... 73

REFERENCES ..... 76

**VITAE ..... 80**

# LIST OF TABLES

Table 3.1 Chemical composition and main alloying elements of 5052 Aluminium alloy (weight %) were measured using spark spectroscopy ..... 36
Table 3.2 Chemical composition and main alloying elements of ASTM A516 grade 70 (weight %) were measured using spark spectroscopy ..... 36
Table 3.3 Mechanical and Physical properties of Al 5052 and ASTM A516-70 steel [55]..... 36
Table 3.4 Experimental Matrix..... 41
Table 4.1: Top view of FSDC samples at different welding and rotational speeds..... 48
Table 4.2: Surface Roughness measurements for the FSDC samples ..... 50
Table 4.3: The average grain size of steel at different rotational speeds (rpm)..... 54
Table 4.4: The average grain size at different travel speeds (mm/min)..... 54
Table 4.5: The thickness of the diffusion layer at the joint interface ..... 58
Table 4.6 : Average Hardness values at the cross section of a cladded sample. ..... 64
Table 4.7: The polarization parameters of all FSDC samples after 504-hour immersion in 3.5 wt.% NaCl..... 72

# LIST OF FIGURES

Figure 1.1: Laser cladding process [9]..... 5
Figure 1.2: Weld overlay cladding [7]..... 5

Figure 1.3: The processing procedure of roll cladding [8] ..... 7
Figure 1.4: Schematic diagram of friction stir welding process (a) Butt FSW [16] (b) Lap FSW [11]. ..... 12
Figure 1.5: Friction stir diffusion cladding process the entire surface ..... 13
Figure 2.1: illustration of HFDB process of lapped sheets [39] ..... 27
Figure 3.1 : (a) FSW machine RM-1, (b) Clamping system, (c) Clamped sample ..... 38
Figure 3.2: FSDC tool body, tool pin and shoulder. (All dimensions are provided in mm) ..... 40
Figure 3.3: Tensile test machine ..... 44
Figure 3.4: lap joint schematic and tensile shear specimen (dimensions in mm). ..... 44
Figure 3.5: Electrochemical cell and corrosion test setup ..... 45
Figure 4.1: Surface defects of FSDC samples a) Lack of fill at sample A100, b) Voids formed at sample A 150 ..... 49
Figure 4.2: Axial Force at different FSDC process conditions. ..... 49
Figure 4.3: Surface roughness of cladded samples at 50 mm/ min welding speed and different rotational speed of a) 1000 b), 500, c) 250 (RPM) ..... 50
Figure 4.4: Optical microscope image of ASTM A516-70 base material ..... 52
Figure 4.5 : Mechanical mixing of clad Aluminum and Steel at 1000 RPM and 50mm/min ..... 52
Figure 4.6: Pearlite lamellar (layered) structure at 1000 RPM and 50mm/min. ..... 54
Figure 4.7: SEM images of all cladded samples at interface a) A50, b) A100, c) A150, d) B50, e) B100, f) B150 and g) C50. ..... 56
Figure 4.8: EDS analysis - line scan of sample B50. ..... 57
Figure 4.9: SEM images reveal the effect of rotational speed on steel grain size at fixed welding speed of 50 mm/min and a) 1000 rpm, b) 500 rpm, and c) 250 rpm ..... 59
Figure 4.10: SEM images reveal the effect of welding speed on steel grain size at fix rotational speed of 1000 and a) 50 mm/min, b) 100 mm/min, c) 150 mm/min. ..... 59
Figure 4.11: Shows the XRD patterns of the interface for all cladded samples and the diffraction lines for Al, Fe, and $Al_{13}Fe_4$ phase. ..... 61
Figure 4.12: Hardness distribution along the cross section of the clad sample A50. ..... 63
Figure 4.13 : Hardness profile along the cladded sample cross section ..... 63
Figure 4.14:The effect of traveling speed on the fracture load at rotational speed of 1000 and 500 rpm. ..... 66
Figure 4.15: The effect of rotational speed on the joint fracture load at fixed travel speed of 50 mm/min. ..... 66
Figure 4.16: Tensile shear test specimen ..... 67
Figure 4.17:The tensile shear failure locations at samples B50, B100 and B150 ..... 67

Figure 4.18: EIS Nyquist plots after immersion duration of 24 and 504 hours for all cladded samples produced at different FSDC process parameters. .. 70
Figure 4.19: EIS Nyquist plot for the effect of rotational speeds on corrosion resistance after a) 24 H, b) 504 H ..... 71
Figure 4.20: Shows the potentiodynamic polarization curves of all cladded samples at room temperature. ..... 72

# LIST OF ABBREVIATIONS

| | | |
|---|---|---|
| SAW | : | Submerged arc welding |
| TIG | : | Tungsten Inert Gas |
| FSW | : | Friction Stir Welding |
| FSDC | : | Friction stir diffusion cladding |
| TWI | : | The Welding Institute |
| FS | : | Friction Surfacing |
| FSLW | : | Friction Stir Lap Welding |
| FSP | : | Friction Stir Processing |
| MP-FSP | : | Multi Pass Friction Stir Processing |
| GMAW | : | Gas Metal Arc Welding |
| GMAW | : | Gas Metal Arc Welding |
| TEM | : | Transmission Electron Microscope |
| EDX | : | Energy Dispersive X-ray |
| SEM | : | Scanning Electron Microscope |
| IMCs | : | Intermetallic Compounds |
| HFDB | : | Hybrid Friction Diffusion Bonding |
| AES | : | Auger Electron Spectroscopy |

| | | |
|---|---|---|
| SAM | : | Scanning Auger microscopy |
| RPM | : | Revolution Per Minute |
| OM | : | Optical Microscope |
| XRD | : | X-Ray Diffraction |
| CNC | : | Computer Numerical Control |
| OCP | : | Open Circuit Potential |
| SCE | : | Standard Calomel Electrode |
| E-Chem | : | Electrochemical |
| HFDB | : | Hybrid Friction Diffusion Bonding |
| HAZ | : | Heat Affected Zone |
| BM | : | Base Material |

# ABSTRACT

Full Name : Almigdad Babiker Hamid Ibrahim

Thesis Title : Developing Friction Stir Diffusion Cladding (FSDC) Process

Major Field : Mechanical Engineering

Date of Degree : May 2017

Cladding is used either to protect the surfaces of an equipment from corrosion or to enhance surface wear resistance. Most cladding processes are performed using fusion methods, where excessive heat input, melting and solidification during the fusion process can result in cracking, porosity formation, distortion, and development of tensile residual stresses in the cladded workpiece. Such defects increase the risk of failure in the clad layer or the substrate. To overcome the abovementioned fusion cladding drawbacks, solid-state cladding technologies can be utilized.

In this study, a solid-state friction stir diffusion cladding (FSDC) process has been developed successfully based on friction stir welding (FSW) principles. The developed process has been implemented for cladding ASTM 516-70 pressure vessel steel with a thin aluminium alloy (5052-H32) sheet for corrosion protection. The effect of process parameters; i.e. tool rotational and welding speeds, on microstructure was studied using Optical Microscope (OM) and Scanning Electron Microscope (SEM) to identify the microstructure, chemical composition and physical properties of the diffusion bonding between the clad material and the substrate. Moreover, XRD was used to identify the developed intermetallic compounds at the interface. The mechanical properties and corrosion resistance of the cladded steel has been also investigated to identify the effect of process parameters and define the optimum conditions. It is very important to control all the process parameters like; pin depth, rotational and travel speeds, and tool tilt angle

in order to reduce the thickness of the intermetallic compounds and enhance the joint quality. It is found that a combination of high rotational and high travel speeds result in surface defects such as lack of fill and voids on the surface, while low rotational and high travel speeds result in weak bonding at the interface with disbandment of the cladding material. Similarly, advance per revolution (APR) influences the surface roughness as well as the corrosion resistance. As APR increases the surface roughness increases too and vice versa. Improved mechanical and corrosion properties were obtained at a optimum combination of rotational and travel speeds of 500 RPM and 50 mm/min respectively.

# ملخص الرسالة

**الاسم الكامل**: المقداد بابكر حامد إبراهيم

**عنوان الرسالة:** تطوير عملية الكسوة بإستخدام طرق الإحتكاك التحريكي

**التخصص:** الهندسة الميكانيكية

**تاريخ الدرجة العلمية**: مايو 2017

تستخدم الكسوة لحماية أسطح المعدات المصنعة من الحديد من الصدأ أو التآكل الناتج عن إحتكاك الأسطح ببعضها البعض. عادة يتم تنفيذ معظم عمليات الكسوة باستخدام تقنيات الإنصهار ، حيث تتسبب الحرارة المفرطة بذوبان المادة و صهرها ، و من ثم تتم عملية تصلب المادة نتيجة للتبريد. أثناء عملية تصلب المادة المنصهرة تنتج بعض العيوب و التشوهات كظهور الشقوق، المسامات و الفراغات ، بالإضافة إلى الإجهادات المتولدة أثناء الإنكماش نسبة لتباين الخواص الكيميائية و الفيزيائية بين المواد. ظهورهذه العيوب في أسطح المعدات يسبب الصدأ الأسطح والتآكل المستمر في طبقة الكسوة و منها للجزاء الداخلية إلى ان تتسبب في فشل المنظومة. للتغلب على العيوب الناتجة عن إستخدام الكسوة بتقنيات الإنصهار المذكورة أعلاه، يمكن استخدام تقنيات الكسوة في الحالة الصلبة.

الهدف الرئيسي من هذا البحث هو، دراسة و تطوير طرق الكسوة بإستخدام الإحتكاك التحريكي لإنتاج طبقة كسوة في الحالة الصلبة تزيد من مقاومة أسطح الحديد للصدأ. تم إستنباط تقنية الكسوة بإستخدام الإحتكاك التحريكي من تقنيات اللحام التحريكي الإحتكاكي . في هذه الدراسة تم تنفيذ عملية الكسوة الإحتكاكية الحركية بنجاح و ذلك بإستخدام صاج رقيق من سبائك الألومنيوم لكسوة أسطح الحديد المستخدم في صناعة أوعية الضغط و حمايتها من الصدأ. تم دراسة تأثير العوامل المتغيرة في التجربة كالسرعة الدورانية و السرعة الخطية على جودة الكسوة و مقاومتها للصدأ بإستخدام التقنيات المجهرية الضوئية و الإلكترونية لتحديد الخصائص الفيزيائية والكيميائية للارتباط بين المادتين و تحديد مدى الانتشار بين عناصر مادة الكسوة و الحديد. تم أيضا إختبار الخواص الميكانيكية ومقاومة الصدأ لضمان جودة عملية الكسوة. إستنادا إلى النتائج تم تحديد الظروف التشغيلية و المتغيرات المثلى التي تنتج طبقة كسوة قوية وفعالة مقاومة للصدأ. قد تم التوصل إلى أفضل النتائج عند استخدام سرعة دورانية قدرها 500 لفة في الدقيقة مع سرعة خطية قدرها 50 مم\ث أو سرعة دورانية تبلغ 1000 لفة في الدقيقة مع سرعة خطية قدرها 100 مم\ ث.

# Chapter 1

# INTRODUCTION

## 1.1 Motivation

Corrosion is considered one of the main causes of failure in engineering components, which are used in industries such as; oil and gas, petrochemical and water desalination, due to their severe corrosive environment. Although corrosion cannot be eliminated, its effects can be reduced using one of the following approaches; (1) implementation of highly corrosion-resistant materials, for example, stainless steel, (2) application of cladding/coatings, which include metallic and organic coatings, as they are applied on the exposed parts or surfaces to protect them from the corrosive environment. (3) Surface modification processes, which alter the surface microstructure to confer higher resistance to these degradation processes. In the later process, surface is treated and not covered, and the modification in surface microstructure and developed residual stresses on the surface increase the surface resistance to corrosion without introducing any foreign barriers. Surface modification processes are utilized to improve the surface properties of metallic parts, such as: wear resistance, corrosion resistance chemical resistance, thermal conductivity, electrical conductivity and hardness [1].

There are several surface treatment processes; for instance, thermal surface treatments are: flame spraying, plasma spraying, arc welding, case hardening, vapor deposition,

mechanical plating and cladding technique. Usually, the weld cladding technique is used either for the sake of manufacturing or reconditioning parts [2]. Cladding is achieved by employing a layer (coating) of required properties on the surface of an inexpensive material to improve its surface characteristics [3]. Using cladding techniques would result in enhancing surface durability, strength, appearance at a reduced cost.

Effective barriers of alloy cladding and coatings are commonly used to protect surfaces of existing equipment; made from carbon steel, from corrosive environments; e.g. wet $H_2S$, in oil production facilities, and thus prevent corrosion damages. Some oil and gas companies, use corrosion-resistant alloy cladding for pipes, valves, flanges, bends, risers and fittings; this alloy cladding process is commonly applied using the fusion weld overlay methods, which is one of conventional cladding techniques. According to the utilized technique for metals cladding, most problems are resulting from: 1) metallurgical changes and poor bonding at the interface between the substrate and the cladding material, 2) porosity, 3) distortion of the workpiece due to excessive heat input, 4) dilution of deposited cladding metal and the substrate material [3].

Moreover, Fusion cladding processes develop high residual stresses, where post heat treatment is required to relief them. These defects will cause failure within short life service. To overcome these drawbacks of fusion cladding, a new solid-state cladding process for carbon steel with corrosion resistance light alloy to mitigate corrosion problems, using economical and environmentally friendly techniques, is proposed and developed. Some researchers like [4] and [5] have suggested the using of FSW for a cladding process.

## 1.2 General Background

### 1.2.1 Definition of Cladding

The term cladding or hard-facing is defined as: the deposition of one material over another to provide skin or layer intended to improve the surface properties of the substrate material and protect it from corrosion and/or wear. Generally, the term cladding in manufacturing industry is referred to, roll cladding, explosive cladding, sheet cladding, or braze cladding [1].

The main cladding techniques are classified into: conventional, and non- conventional cladding. Most of the conventional techniques are based on fusion process such as: laser cladding, weld cladding, spark plasma sintering. While the non-conventional techniques are based on diffusion process such as: roll cladding and friction surface cladding.

### 1.2.2 Conventional cladding techniques

**Laser cladding** is a process used to fuse another material (powder form), with different metallurgical properties on a substrate, using a laser beam, as illustrated in Figure 1.1. In order to maintain the original properties of the coating material, a very thin layer of the substrate is melted to achieve metallurgical bonding with minimal dilution of added material and substrate [6]. Laser cladding process consists of two essential parts [3]:

1) Melt pool formation and fusion by a moving laser beam;
2) Supply of cladding material to the substrate.

**Weld overlay cladding** techniques are classified as a fusion cladding technique. Basically, weld overlay is based on deposition of the molten welding wire or electrode

material on top of the substrate. This method has been used in various industries such as automotive, aerospace, electronics, shipbuilding, offshore, railway. Predominantly, the surface is wrapped (coated) by a dissimilar clad layer to improve the lifetime of the product [7]. In weld overlay cladding the thickness of the deposited metal is greater than or equal 3 mm (1/8 in) [8]. Usually, Submerged arc welding (SAW) is used to perform weld cladding but other different techniques can also be used. Figure 1.2 presents weld overlay pipe cladding using a hot wire Tungsten Inert Gas (TIG).

Most Cladding/Coating techniques and surface modification processes such as high-energy laser melt treatment, high-energy electron beam irradiation, plasma and thermal spraying involve the solidification of the liquid phase clade created at elevated temperatures to form a surface layer/coating. The solidification/cooling rate must be well controlled to produce the required microstructure, mechanical properties and performance of the modified surface. However, several limitations must be considered for weld overlay cladding such as: required clad thickness and welding position. For instance, submerged arc welding can only be used in flat position. In addition to that, most weld overlay procedures have considerably greater dilution [8]. It was also reported that, most of the Submerged arc welding parameters that affect dilution in weld cladding applications are not well controlled such as: current density, polarity, electrode size and travel speed [8].

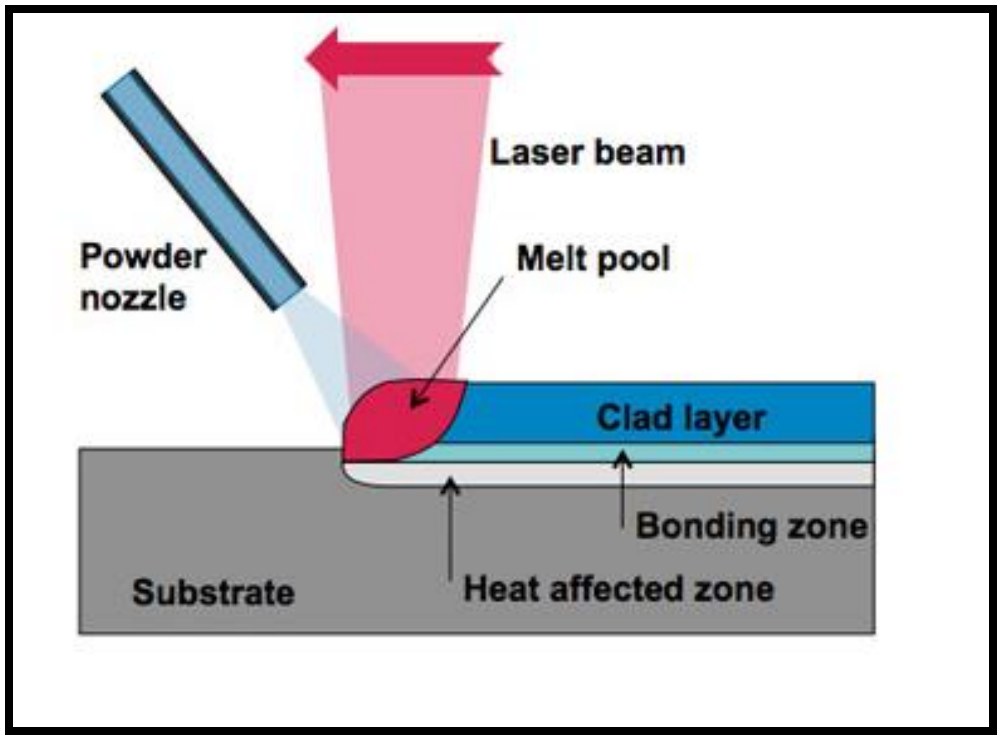


**Figure 1.1:** Laser cladding process [9]

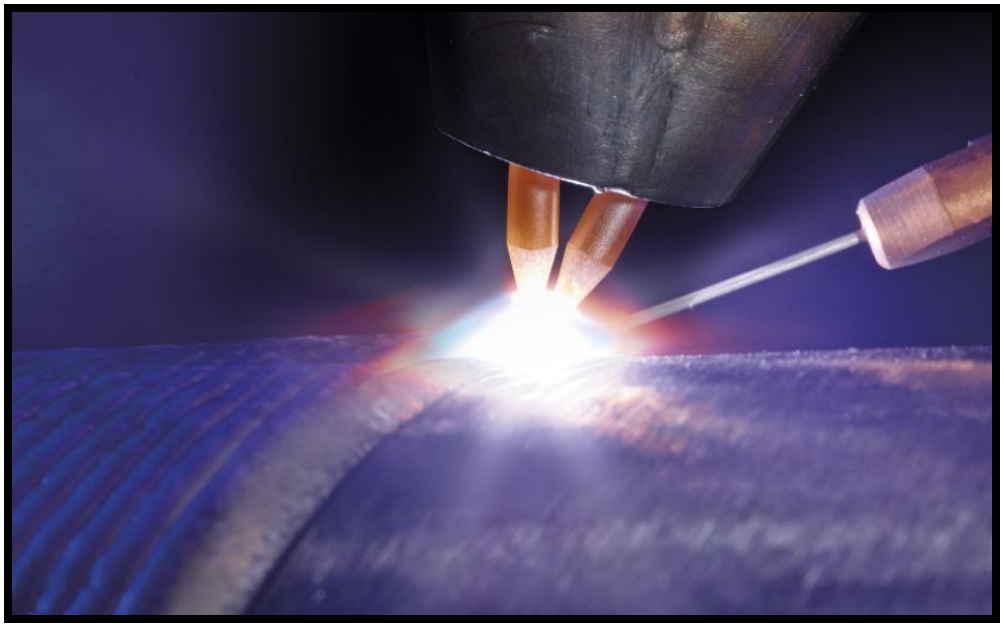

**Figure 1.2:** Weld overlay cladding [7]

### 1.2.3 Non-conventional cladding techniques

**Roll cladding** is achieved by passing a stack of dissimilar metal sheets, plates or strips through a pair of rollers to achieve proper deformation that promotes a solid-state bonding between the metal pieces as illustrated in Figure 1.3.

Fusion-cladding processes have many limitations that arise from the excessive temperatures buildup during the process, as was mentioned before. Moreover, Fusion cladding processes develops high residual stresses, where post heat treatment is required to relief them, this post heat treatment will increase the cost significantly [10]. Moreover, some of the techniques; like laser surface cladding, requires sophisticated and expensive systems, while others like overlay welding may need skilled technicians and has limited clad deposition rates. Deposition rate has a large impact on cost especially when dealing with large surfaces. Therefore, low clad deposition rate will result in reducing the effectiveness of the process. Issues associated with fusion cladding techniques mentioned above can be avoided if the surface modification or cladding occurs in a solid-state or at temperatures below the melting point of the substrate and cladding materials.

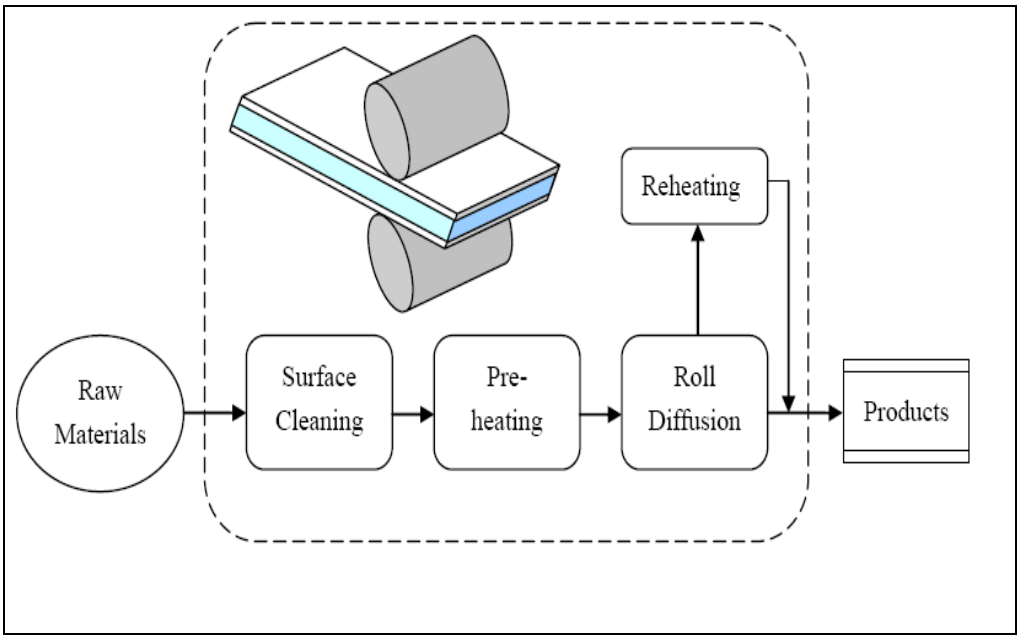


**Figure 1.3: The processing procedure of roll cladding [8]**

### 1.2.4 Materials used in cladding process

Usually, the selection criteria of the substrate metal depends on the required properties for a specific application. For instance, steel is commonly used as a substrate material when strength is required. On the other hand, materials used for cladding are chosen based on many factors that include but not limited to; application, cost, availability, manufacturing parameters, mechanical properties, thermal and electrical properties, corrosion resistance and appearance [8].

In general, metallic cladding materials for corrosion control can be classified as: noble metals, corrosion barrier system, complex multilayer system and sacrificial metals. For example, inexpensive substrate material is covered with a noble metal, such as copper, to provide corrosion resistance to the base metal. Most common types of noble metals used in cladding are: stainless steels (304), high-nickel alloys (Inconel 625), aluminum alloys, copper lead, bronze and brass [8], [11].

Sometimes corrosion barrier system consisted of two or more metals to provide a corrosion barrier system. This type is frequently used where cavities produced by corrosion must be avoided, for example, low carbon steel and stainless steel are susceptible to localized (pitting) corrosion in chloride environments [11]. In some applications, materials could be exposed to dual environment and a single material may not be applicable for this condition. For instance, a corrosive environment could surround one side while the other side is exposed to different medium (i.e. heat), in this case a complex multi-layer system can be used. Small battery cans and caps is an example for complex multi-layer systems [8].

However, Magnesium, zinc, and aluminum, are classified as sacrificial metals. This metal placed in the active segment of the galvanic series and they have been used extensively for corrosion protection. The position of the sacrificial metal in the galvanic series is very important factor in the design of a system [8], [9].

Aluminum has excellent corrosion resistance resulted from its ability to reacts quickly with oxygen to form a hard-passive layer of aluminum oxide, which prevents additional corrosion to occur. In addition to that, aluminum alloys have high strength to weight ratio compared to the other metals, also they are easy to manufacture and have good appearance. Usually, for cladding process, aluminum is used in form of an alloy with magnesium and manganese. In this study, aluminum is selected due to its low cost and good corrosion resistance.

### 1.3 Problem description

Using the fusion cladding techniques for joining dissimilar materials may result in many defects and it is considered very challenging due to the difference between the substrate and clad materials in both physical and mechanical properties such as: melting temperature, thermal expansion and solidification. Therefore, in view of the known limitations of the existing cladding and coating techniques, and the advantages of Friction Stir Welding (FSW) and Friction Stir Diffusion Cladding (FSDC), it appears that FSDC is a viable solution for metal cladding applications. This work presents the process and the results of performing successful cladding of aluminum (5052-H32) to ASTM A516-70 pressure vessel steel using the relatively new friction stir diffusion cladding (FSDC) process.

## 1.4 Friction Stir Diffusion Cladding (FSDC)

Friction stir diffusion cladding (FSDC) is a new technique that involves processing of the clad material in a solid-state fashion. The friction between the tool and the cladding sheet results in heat generation, which softens and plasticizes the cladding material, while the tool axial force will facilitate the diffusion at the interface between the cladding material and the substrate. FSDC process is based on the basic principles of friction stir welding.

Friction stir welding (FSW) was developed by The Welding Institute (TWI) in the United Kingdom [12] in late 1991 as a further development of friction welding technology to overcome welding problems associated with aluminum alloys. Although FSW was initially developed for aluminum alloys, the recent development in tool materials made it possible for welding / processing of high melting temperature metals and alloys, such as steel, copper, titanium and other metals and alloys as well as dissimilar metals.

Different industries, like, aviation, automobile, railways, and many others have used FSW techniques. Special attention from the automobile industry was given to this process to utilize friction stir spot welding to replace resistance spot welding, also joining aluminum to steel in order to reduce the vehicle frame weight while maintaining strength, as it has significant impact on fuel consumption. In addition, many researchers worked on producing Aluminum to steel lap joints and producing laminated Aluminum steel composite [13]–[15]

In FSW process, a rotating shouldered pin tool is inserted into a butting or lapping substrate, and then traveled along the joining line; to produce the joint, as shown in Figure 1.4. The friction between the tool and the workpiece results in localized heating,

which softens and plasticizes the material in contact with the tool. Moreover, the materials are moved from the front to the backside of the pin; thus, the material undergoes intense plastic deformation and mixing, which results in significant grain refinement, densification, and homogeneity of the processed zone.

Cladding carbon steel with suitable clad material using FSDC can be closely presented as performing friction stir lap joint (Figure 1.5), but the tool processes the entire surface of the sheet instead of processing the joining area. In FSDC, a thin sheet (cladding material) is securely clamped on the top of the substrate, so no relative movement can take place between them, and then a rotating FSDC tool is plunged and directed along the surface of the cladding material / desired direction to cover the region of interest. For FSDC tool with pin, penetration will not exceed the cladding sheet thickness to reduce the amount of heat generated at the interface and mechanical mixing between the cladding l and substrate materials, as well as decreasing the tool pin wear. An Illustration of FSDC process is shown in Figure 1.5.

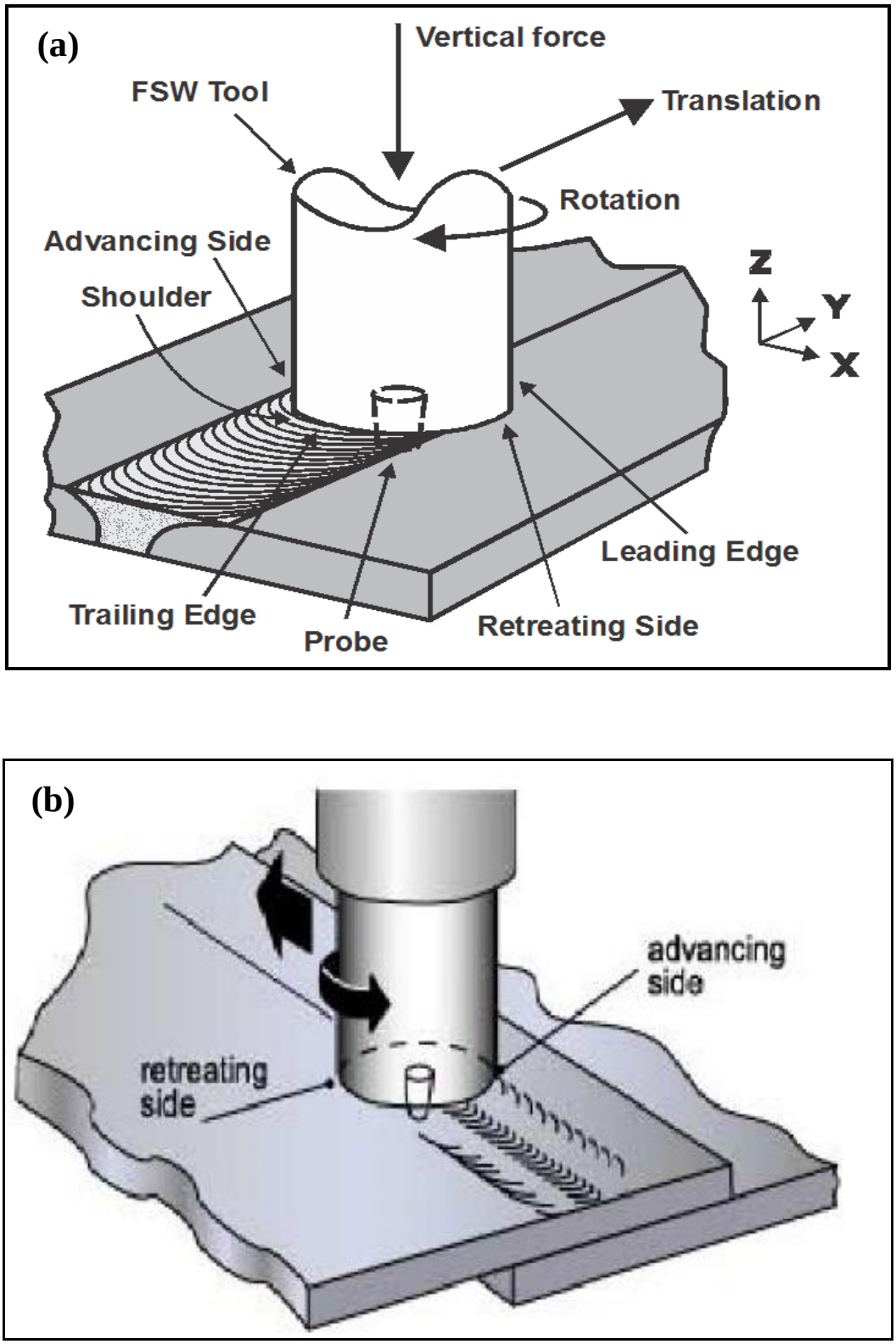


**Figure 1.4:** Schematic diagram of friction stir welding process (a) Butt FSW [16] (b) Lap FSW [11].

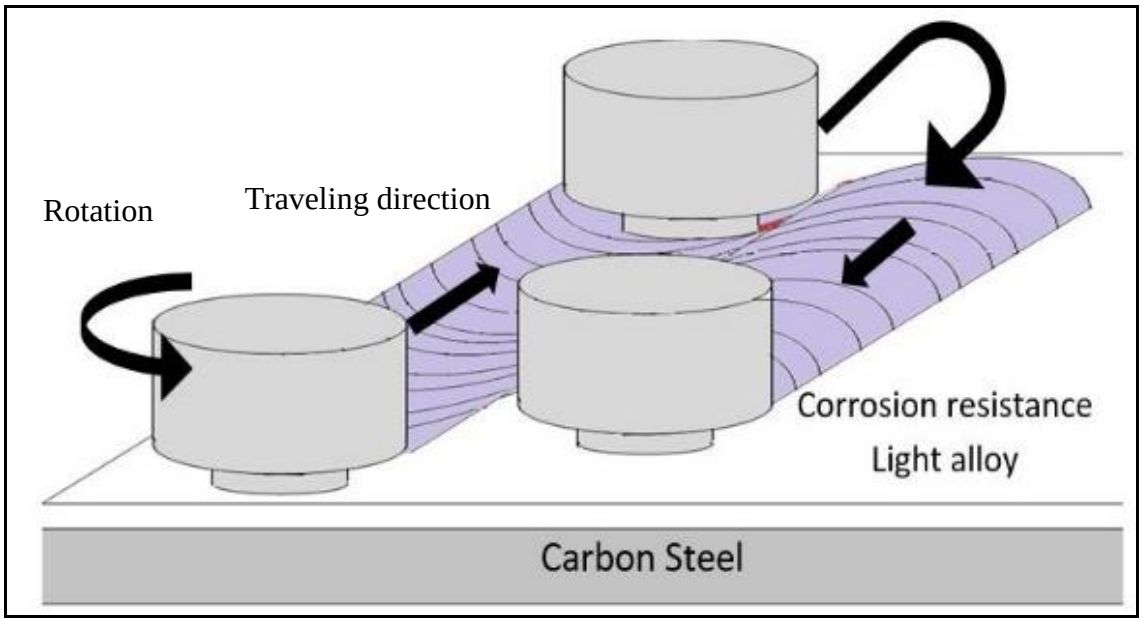


**Figure 1.5: Friction stir diffusion cladding process the entire surface**

## 1.5 Main advantages of FSDC

Since FSDC is based on FSW principles and both processes are in the solid state, FSDC is an environmentally friendly process, as no toxic fumes are generated and it consumes less energy compared to the other fusion or surface modification techniques, i.e. laser cladding/processing, plasma transferred arc welding, and atmospheric plasma spraying. In addition to that, no filler materials or consumables are required, which can reduce the process cost significantly [12]. Moreover, FSW has lower heat input, therefore the residual stresses are lower compared to the other fusion cladding processes. Usually, FSW is an automated process which doesn't require a qualified welder. Since this process does not contain filler material, it allows weight reduction, it helps in reducing the fuel consumption. Also, FSW process was successfully used for various welding positions [12], [14].

Similar to FSW, FSDC has many advantages that arise from the low heat input, these advantages include but not limited to: 1) Metallurgical benefits, since no bulk melting takes place, this process allows dissimilar joining of materials. The absence of melting results in the absence of dilution as well as lowering the residual stress levels since solidification shrinkage does not occur. Also, less surface post-processing requirements.

## 1.6 Objectives

The proposed research focuses on developing solid-state cladding process for carbon steel using FSW principles and selecting the process parameters to produce an effective corrosion-resistant cladding suitable for use in water desalination, petrochemical and oil and gas industries. Achieving the objectives will result in introducing a new effective and

low-cost cladding technology that can help in mitigating corrosion problems at a lower cost. The specific objectives are the following:

1- Develop an experimental setup of the friction stir diffusion cladding (FSDC).
2- Study the influence of FSDC parameters, i.e. tool rotational and welding speeds, on microstructure, mechanical properties as well as corrosion resistance of the cladded steel.
3- Selecting the process parameters i.e. tool rotational and advancing speeds to achieve the optimum mechanical and corrosion resistance properties.

In the proposed work, cladded carbon steel samples with the selected aluminum alloy (Al 5052-H32) are fabricated using different process conditions and tested for microstructural, mechanical, and corrosion performance. First, the mechanical and microstructural properties of the produced samples are evaluated to optimize the processing conditions. Next, corrosion tests are performed on the cladded samples to evaluate the corrosion resistance of the friction diffusion cladded steel in 3.5% wt./volume NaCl electrolytic solution.

The experimental results are analyzed to establish the relationship between the process parameters and the performance (mechanical and microstructural) of the produced samples. Moreover, the research findings will help identify the best FSDC process parameters for cladding selected carbon steel and aluminum alloy.

## 1.7 Organization

This thesis includes five chapters organized as follows: chapter one, covered an overview of the research work and its objectives. Followed by literature review, which covers the state of the art in the field of friction stir welding, processing and cladding. Research methodology, experimental setup, equipment's and tool design for friction stir diffusion cladding process are presented in chapter three. Chapter four includes the results and discussion of microstructure analysis as well as the mechanical and corrosion tests performed on the cladded samples to examine the quality of the clad joint. Finally, chapter five contains research conclusions and recommendations.

# Chapter 2

# LITERATURE REVIEW

This chapter highlights the state of the art on the experimental research of friction stir, welding, processing and cladding that will assist the interpretation of the experimental results.

## 2.1 Friction Stir Lap Welding

Friction stir welding process has been used to join similar and dissimilar materials such as aluminum alloys and steels with a stronger bond compared to conventional welding processes. The need for reducing structure weight in some applications such as aerospace and automotive body resulting in increasing the utilization of the lap joining of aluminum and titanium alloys for space shuttle and cars fabrications [17].

Friction stir diffusion cladding process (FSDC) is very similar to friction stir welding of lap joint as described in section 1.4. FSDC can be performed using either pinless tool or tool with pin depending on the thickness of the cladding material used. However, when using tool with pin for FSDC the penetration of the pin should not exceed the clad material thickness for the reasons mentioned earlier.

Many studies have been conducted on the joining of different alloys, such as aluminum or Copper, with steel using FSW to produce butt or lap joints. Yet, few studies have been reported on Al to-steel lap joints [10], [15], [18]–[22].

Elrefaey et al. [18] investigated the ability of joining pure aluminum plate to low carbon steel plate by using friction stir lap welding (FSLW). Also, they studied the relationship between the joint strength and the process parameters. They found that, the depth of the probe tip into the steel surface effect the joint strength significantly. For instance, the joint was failed under low applied load when the probe tip did not reach the steel surface. Conversely, small penetration of the pin tip toward the steel surface increasing the joint strength considerably. In addition, the authors found that the joints formed at high rotation speeds between 1500 and 2502 RPM had higher strength compared to those formed at a rotation speed of 1002 RPM. They also observed that, the Fracture of the joints formed at higher rotation speeds occurred mainly in the layered structure (IMCs), probably owing to the formation of intermetallic compounds such as $Al_5Fe_2$ and $Al_{13}Fe_4$. The authors [18] suggested that it is possible to achieve quality joints between Al and steel using FSW by carefully controlling the pin depth to avoid the formation of an intermetallic-rich layered structure.

Soltani et al. [19] studied the effects of welding speed, tilting angle and rotational speed on the mechanical properties of FSW lap joint between austenitic stainless steel and aluminum alloy. They found that, either increasing the rational speed or decreasing the tool travel speed will reduce the shear strength of the joint significantly due to the high heat input, and defect formation in the weld zone; such as cavities and flash. At 80 mm/min welding speed and a rotational speed of 1000 rpm the authors reported a

maximum fracture load of 7750 N, while the joint fracture load reduced to 3350 N when 2000 rpm was used. Increasing the tool tilt angle was also found to negatively affect the shear strength of the joint due to the high plastic deformation on the weld zone. The authors reported that, the joint strength improved and then degraded with increasing the tilting angle. The fracture load reduced from 7750 N to 4180N when the tilting angle increased from 1.5 to 2.5 degree while fixing other conditions. The formed flash around the weld zone increased with the heat input. Soltani et al. [19] also found that the hardness of austenitic stainless steel at the joint was higher than the base metal; 365 Vickers at the interface and 305 Vickers at the base metal. It was explained that the increase occurred due to: 1) the high work hardening, and 2) the formation of intermetallic phases, on the other hand, no changes were reported for aluminum alloy. However, the author [19] findings contradict the findings of Elrefaey et al. [18], because of the different of the materials they used.

Elrefaey et al. [23] investigate the feasibility of FSLW of pure aluminum plate and zinc-coated steel sheet. They found that the quality of the joint strength depends significantly on the depth of the probe tip into the steel surface similar to their earlier findings in [18]. For instance, the joint was failed under low (200 N) applied load When the probe tip did not reach the steel surface. Conversely, small penetration of the probe tip toward the steel surface increasing the joint strength considerably. Likewise, the effect of the rotational speed and the traverse speed on both the microstructure and mechanical properties was studied, the authors found that, strength of the joint improved by increasing the rotation speed and slightly decreasing the travel speed similar to what has been reported by [18]. In addition to that, the authors compared the bonding strength of the weld joint of

aluminum to steel with zinc-coating versus aluminum to steel without zinc coating, they conclude with the fact that bonding strength was higher at all bonding parameters for aluminum sheet joint to steel with zinc-coating, thus they proposed the advantageous of using zinc coating and its effect on joint strength [23].

Chen et al. [24] studied the feasibility of performing (FSLW) of low-carbon zinc-coated steel and AC4C cast aluminum alloy at constant rotational speed of 1500 RPM and different welding speeds (60,80,100 and 120 mm/min). They found that, the mechanical properties (tensile properties and fracture locations of the joint) were effected significantly by the welding speed. At lower welding speed of 60 mm/ min the joints fractured at the interface and the shear strength was 50 MPa. On the other hand, at welding speed of 80 mm/min or higher (100 and 120 mm/min), the tensile strength of the joint was equal to that of zinc-coated steel, the maximum fracture strength was 331.8 MPa when 100 mm/min welding speed was used.

Chen and Nakata [15] investigate the effect of the steel surface conditions on FSLW of Al to steel. Different conditions were considered, including rough, smooth and zinc-coated surfaces. The results showed that the surface state of steel has a significant effect on the mechanical properties of lap joints welded at the same welding parameters similar to what has been reported by [23]. In addition to that, the presence of a zinc coating over the steel increased the weldability of Al onto steel and it had the largest fracture strength. For the solid-state bonded joint of dissimilar metals, there are two main factors controlling the joining performance, one is the intimate contact between aluminum and steel, and the other is the microstructure, particularly the formation of intermetallic compounds.

The effect of FSW tool plunging depth, travel speed and rotational speed on the shear strength of the lap joint of A5083 Aluminum alloy and SS400 steel was studied by Kimapong and Watanabe [21]. They found that, the shear strength of the lap joint was decreased with either increasing of tool rotational speed or reducing the tool travel speed, which was due to the formation of $FeAl_3$ intermetallic compound layer at the joint interface. $FeAl_3$ phase is brittle, thus it reduces the mechanical properties of the joint. Increasing tool rotational speed will increase the heat input and the thickness of the intermetallic layer formed, therefore reduces the joint strength in contrast to what has been reported by Elrefaey et al. [15 - 21]. Although, the joint shear strength was increased with increasing of the tool travel speed, high travel speed such as 85.8 mm/min resulted in incomplete joint at the interface [21]. The authors, reported the maximum joint strength of 130 MPa when 10 mm pre-hole diameter was used with the following welding process parameters of; 225 RPM rotational speed, 44 mm/min welding speed, 0.1 mm over plunging inside the substrate and 1 $^{o}$ tilting angle using unthreaded FSW tool with 5 mm pin diameter and 3 mm long. The effect of pin tool plunging depth was also studied by Kimapong and Watanabe [21], and they found that the more plunging depth the thicker the intermetallic layer at the interface and more likely to have imperfect weld joint. This result shows strong agreement with Elrefaey [18] results.

Kimapong and Watanabe [21] also reported the fracture behavior when different rotational speed was used. At high rotational speed of (1240.2 RPM), the joint was failed by brittle fracture located in the intermetallic layer. On the other hand, ductile fracture was found at the aluminum side when low rotational speed of (225 RPM) was used.

In another work of Kimapong and Watanabe [25], the effect of pin tool diameter, tilting angle and pre-hole on Friction Stir Lap Welding of SS400 steel and 5083 Aluminum was investigated. They indicated that, when the tilt angle or the probe diameter increased, the joint shear strength decreased which is strongly agree with the results reported by A. Soltani et al. [19]. Increasing the tool title angle produce a thick intermetallic compound layer of ($Fe_2Al_5$) at the weld interface. They also found that, the larger the pin diameter the thicker the thickness of ($FeAl_3$). intermetallic compound layer. Moreover, larger voids had appeared at the weld interface; affecting the quality of the joint. On the other hand, they reported that application of pre-hole on the plunging side of Al sheet enhanced the shear strength of the joint because it helps to reduce the quantity of intermetallic phase formed at the joint interface [25].

Chen and S. Yazdanian [26] investigate the effect of hook formed through FSLW on the strength of the weld joint of Aluminum to Aluminum, Magnesium to Magnesium. Also, and aluminum to steel. The fracture behavior during the mechanical testing was studied by preforming microstructure analysis of the interface. They found out that, controlling the plunging depth is very important in order to form a mixed stir zone (MSZ) and reasonable strength.

Prasad Rao Kalvala et al. [27] were successfully studied the seam welding of multi-layered similar and dissimilar metallic sheets of AISI 303, Ni- based alloys, C-Mn steels, Ti6A14V, CP Cu, CP Ni and AA6061 by using a pinless tool. Defect free and bonded samples of multi layered similar and dissimilar metallic sheet were produced using a solid-state seam welding technique. The authors found that, the tensile shear of the seam welds was stronger than the base metal counterparts, and the bonding at the sheets

interface was referred to the localized stick and slip at the interface as well as the diffusion and dynamic recrystallization with finer grains compared to the base material [27].

Zhao et al. [28] successfully cladded AZ31B magnesium alloy with 1060 Aluminum using multi pass friction stir processing (MP-FSP) and studied the microstructure and mechanical properties of the interface. They found that, the formation of the intermetallic compounds (IMCs) is controlled by the diffusion time and heat input. Moreover, the thickness of the intermetallic layer and the hardness were found to increase with decreasing the welding speed. The joint tensile shear strength was found increasing with increasing the thickness of the IMCs layer at the interface. For instance, tensile shear strength increase as the thickness of the IMCs layer increase too. However, this result was found reverse to what has been reported earlier by the other researches [19], [21], [29].

Shen et al. [10] introduced the first comparison between friction stir lap welding (FSLW) of pure copper cladding sheet to pressure vessel A516-70 steel plate versus cladding by pulsed current gas metal arc welding (GMAW). The FSW tool used was made of Co–WC cermet with 2.1 mm pin long, 5 mm diameter and tapered geometry as well as 12 mm shoulder. The applied process parameters were 1120 RPM rotational speed and 31.5 mm/min welding speed together with 2.5$^{o}$ tilt angle. The authors reported that, the FSW process produce finer grains structure in copper cladding with free cracks bonding and no dilution was found, however Nano-pores was detected at the interface. On the other hand, copper cladded steel using GMAW included many cracks on the surface referred to high thermal stresses, in addition to the diffusion of manganese and silicon into the copper

cladding attributed to the higher temperature executed, and liquid permeation of copper inside the substrate.

In another interesting work of Y. Gao et al. [30] were they successfully produced a FSLW of brass (Cu – 40Zn) to plain carbon steel (S25C) at a constant plunging force of 9.8 kN and 3° tool tilting angle. They investigated the relationship between the heat input and different welding speeds ((250, 400, 500 and 600 mm/min) and rotation speeds (1000, 1250 and 1300 RPM)). Also, they studied the influence of the welding speed on mechanical and microstructure properties of the lap joint. The authors found that, at low heat input no joint was formed due to the insufficient amount of heat to generate diffusion bonding on the interface, a groove defect and large protrusions were formed when high heat input was used. Transmission electron microscope (TEM) and energy dispersive x-ray (EDX) results revealed the incidence of diffusion bonding with no evidence of forming any intermetallic compounds at the interface joint at all selected parameters. As welding speed increased, the tensile shear strength of the joint decreased significantly. On the other hand, as welding speed decreased the grain size increased and hardness decreased too.

Saeid et al. [31] successfully produced a lap joint of 1060 Al sheet and commercially pure Cu sheet using FSW process, they investigate the influence of welding speed on joint strength and interface microstructure at constant tool rotational speed of 1180 RPM. The results revealed the formation of IMCs at the interface with some microcracks; these cracks were increased as welding speed reduced. Alternatively, some cavities were observed in the interface at high welding speed (118 and 190 mm/min) due to the inadequate heat input. However, free cavities weld joint with few microcracks and

maximum tensile shear strength of (2642 N) was achieved at a travel speed of 95 mm/min.

### 2.2 Friction stir processing (surface modification)

Many researchers have investigated surface modification or metallic matrix formation using Friction Stir Processing (FSP), and studied its effect on mechanical and microstructural properties. Examples are given here to show the successes of FSP in enhancing material properties.

Sharma et al. [32], and Santell et al. [33] studied fatigue performance of a friction stir (FS) processed A356 and A319 alloys. Their experimental results showed that fatigue life was significantly improved owing to grain refinement and removal of the casting induced porosity. Other studies [17, 18] also revealed enhancements of surface wear resistance of many alloy steels, like: SKD61 tool steel [20], and AISI 420 martensitic stainless steel [34].

For hydroturbine applications, Grewal et al. [35] studied the enhancement of cavitation erosion resistance in friction stir processed 13Cr4Ni steel. Their experimental results revealed that cavitation erosion resistance was increased by 2.4 times compared to that of unprocessed steel. The microstructural changes introduced by FSP enhance not only the mechanical properties but also the corrosion performance of some processed alloys. Rao et al. [36] investigated the corrosion behavior of dissimilar aluminum–copper welds produced by gas tungsten arc welding and processed by FSP. Microstructural analysis revealed that the processed welds had uniformly distributed $CuAl_2$ intermetallic particles,

with more uniform distribution of copper in the weldment, which led to the enhancement of weld corrosion resistance.

Using friction surfacing, Rafi et al. [37] produced a defect-free low carbon steel coated with AISI H13 tool steel. The authors found an increase in the hardness of the fabricated samples in the as-deposited conditions, which reached 58 HRC at the coating.

### 2.3 Pinless FSW and Friction diffusion bonding

A few studies were found on the hybrid friction diffusion bonding (HFDB) and pinless friction stir welding (FSW) of similar and dissimilar metals.

HFDB is a relatively new process, it is very similar to friction stir lap welding, but it utilizes a pinless rotating tool (see Figure 2.1). Unlike FSW, no mechanical mixing between lapped sheets takes place, but the rotating tool generates frictional heat and applies forging load on the top sheet, the pressure and heat results in producing diffusion bond between the lapped sheets.

Bergmann et al [38] studied different solid state welding methods for joining copper and aluminum, their study focused on the effect of the utilized technique on electrical resistance of produced joint. The authors used diffusion bonding in vacuumed chamber, hybrid spot friction diffusion bonding, and last friction stir welding. Results indicated that full bond was formed using diffusion bonding after 180 min at 500 ºC, and pressure between 4-6MPa. While in hybrid spot friction diffusion bonding (HFDB), spots were formed in 2 secs, but SEM results did not reveal the formation of diffusion layers between copper and aluminum.

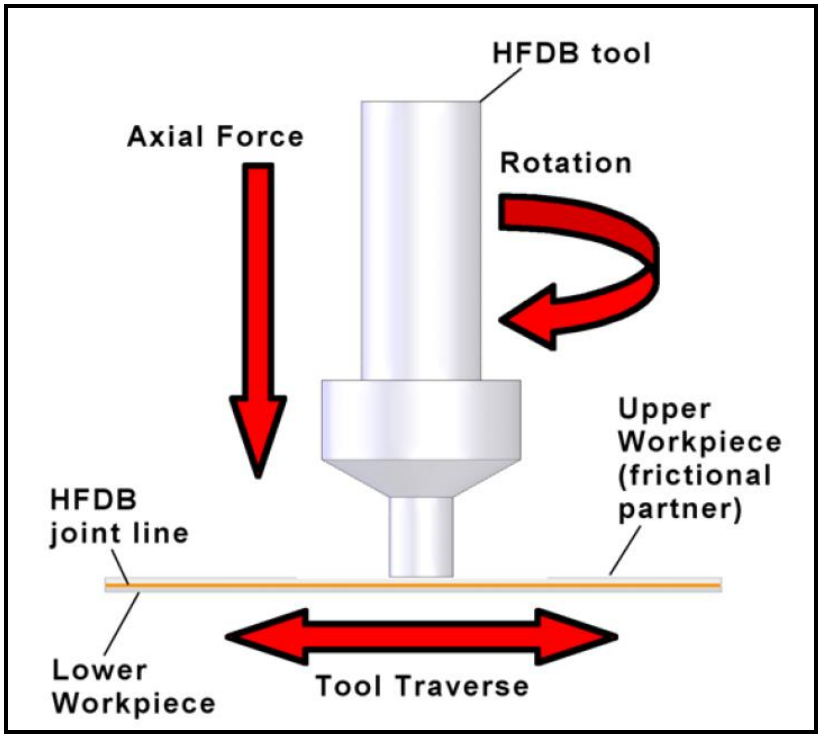


**Figure 2.1: illustration of HFDB process of lapped sheets** [39]

In FSW of thin sheets, number of researchers reported that using conventional friction stir welding tool may result in a defected or low strength joints [25, 26] . Forcellese et al [40] successfully produced friction stir butt welds of thin sheets (0.8 mm) AZ31 magnesium alloy using two different tool shoulder sizes with pin and pinless. In their study, the effect of process parameters on mechanical and microstructural properties were investigated. The authors reported that the pinless tool produced more homogeneous microstructure compared to that obtained using the pin tool one. Although more grain refinement was resulted by the pin tool, cavities and voids were also formed and they were responsible for reducing the mechanical strength of the produced joint. Another investigation on pinless friction stir butt welding was reported by Wenya et al [41]. In their study, the effect of process condition i.e. the rotational and welding speeds on mechanical, microstructural and failure mode of pinless friction stir butt welded thin sheet (1.5 mm) AA2024-T3 was analyzed. Their results showed that joints with defect free and without root flaw and keyhole were successfully produced. A closer process to HFDB is pinless friction stir spot welding, which was developed to mitigate defects generated in conventional friction stir spot welding that affect produced joint strength, such as; keyhole and hook defects.

Bakavos et al. [42] studied pinless friction stir spot welding and high power Ultrasonic Spot welding for joining thin aluminium sheets for automotive industry. The authors were able to produce high strength spot welds with process time of 0.5 sec. The authors also showed that using pinless tool, high lap shear strength of about 3.4 kN in thin aluminium sheet in the range of 1 mm thick, could be achieved with short weld cycle times. In Bakavos et al. [42] work, they investigated the effect of the pinless tool profile

namely flat tool, fluted wiper tools (short and long flute wipers), proud wiper tool, and scroll tool on mechanical properties and material flow. They found that, fluted wiper tools produced the maximum failure loads. Also, flat tools were found able to procedure acceptable strength nonetheless it required more dwelling time to produce joint with the same strength as fluted tools. However, the worst strength was produced by the proud wiper tool.

### 2.4 Corrosion behavior of FSW joints

A number of researchers have studied the corrosion susceptibility of friction stir welded aluminium alloys. Alison Davenport et al. [43] investigated the effect of process parameters on the corrosion sensitivity of AA2024friction stir welds. They found that, increasing the tool rotation speed will cause high cathodic reactivity in the nugget zone because of the precipitation of the S-phase. Another investigation about the effect of FSW process parameters on the corrosion behavior of AA 2024 -T351 aluminum alloy was carried out by Jariyaboon et al. [44]. They found that, the location of corrosion attack is primarily related to the tool rotational speed. For instance, at low rotational speed welds the localized intergranular attack was observed in the nugget zone, while at higher rotational speed it was predominantly detected in the heat-affected zone (HAZ). They also noticed an increase in the cathodic reactivity at the nugget zone as a consequence of the precipitation of S-phase particles, similar to the findings in [41].

Surekha et al. [45] carried out through multipass friction stir process to improve the corrosion resistance of AA 2219-T87 aluminium alloy. They found that, all the processed alloys exhibited superior corrosion resistance compared to the base material regardless of

the process parameters utilized. In addition to that, increasing the number of passes through the friction stir processing found to improve the corrosion resistance significantly. Likewise, it was reported that $CuAl_2$ particles were dissolve during the friction stir processing which decreases the corrosion rates as well as the number of spots available for galvanic corrosion. In another work of Surekha et al. [46], the influence of tool rotational and traverse speeds on the corrosion resistance of AA 2219-T87 aluminum alloy using different corrosion testing methods including: polarization, electrochemical impedance spectroscopy, salt spray, and immersion tests. Their results showed that, the corrosion rate was mostly influenced by the tool rotational speed rather than the traverse speed, which did not affect the corrosion behavior of the processed welds. This was attributed to the dissolution of the intermetallic compounds. Also, they have found that both corrosion resistance and the amount of dissolution particles increased with increasing the rotational speed.

Similarly, Xu and Liu [47] investigated the effect of FSW process parameter on pitting corrosion, and microstructure of 2219-O aluminum alloy. Using scanning electron microscopy along with electrochemical impedance and polarization tests of the weld nugget zone, they found that the processed material exhibit better corrosion resistance compared to the base metal, this result is similar to findings of Surekha et al. [45]. In addition, they conveyed that increasing the rotational speed resulted in decreasing the corrosion resistance. For instance, at welding speed of 80 mm/min the corrosion resistance at 500 rpm rotational speed was higher than that at 600 rpm. Similarly, at low rotational speed of 400 rpm the corrosion resistance reduced tremendously when the traverse speed increased from 60 to 100 mm/min, this result indicates that the corrosion

resistance is highly sensitive to the welding speed which is opposite to the finding of Surekha et al. [46].

Although Xu and Liu [47] shows strong agreement with the results reported by the [45] regarding the relationship between the rotational speed and the corrosion resistance, they showed substantial disagreement with the result reported by Surekha et al. [46] about the traverse speed. Weifeng Xu and Jinhe Liu found that increasing the traverse speed will result in decreasing the corrosion resistance [47]. This contradiction was resulted from the differences in used workpiece thickness and FSW process parameters. For instance, Xu and Liu [47] performed the FSW at 400–600 rpm rotational speed and traverse speed of 60–100 mm/min on14 mm thick material while Surekha et al. [46] processed the sample at a rotation speed of 1600 rpm and a traverse speed of 22.2mm/min on 5 mm thick workpiece.

Grilli et al. [48] also studied the pitting corrosion behavior of Al 2219 alloy in 3.5% NaCl solution as a function of exposure time. Their Energy Dispersive X-ray analysis (EDX), Auger Electron Spectroscopy (AES) and Scanning Auger microscopy (SAM) results displayed the cathodic nature of the Intermetallic compounds (IMCs) with reference to the aluminum matrix.

Surekha et al. [49] investigated the corrosion behavior of AA 2219 aluminium using two different surface treatment techniques FSP and fusion based laser melting. They found that, both surface treatment techniques exhibit similar corrosion resistance, this was attributed to the dissolution of second phase particles in AA 2219 alloy, as a result of that the corrosion performance will enhance significantly. However, the corrosion resistance

was found proportional to dissolution of the second phase in the alloy regardless of what technique have been used. On the other hand, hardness test results reveal that FSP samples show higher hardness compared to laser melted samples which point out that FSP technique has better mechanical properties than laser melting technique [49].

Recently, Qin et al. [50] studied the corrosion behavior of FSW 2A14-T6 aluminum alloy inundated in EXCO solution (mix of 4.0 mole NaCl, 0.5 mole $KNO_3$ and 0.1 mole $HNO_3$) using several electrochemical procedures such as: open circuit potential, polarization and impedance spectroscopy. SEM and EDS were also utilized for investigating the corrosion mechanism. The results reveal that, the friction stir welded samples presented a considerable enhancement in the corrosion resistance with respect to the base metal, and the maximum corrosion resistance was found in the weld nugget. Similarly, the pitting tendency resulted from the superiority of (Al, Cu, Fe, Mn and Si) phase particles as cathodic elements compared to the matrix attributed to its high self-corrosion potential.

Jariyaboon et al. [51] successfully studied the corrosion performance of dissimilar aluminum alloys (AA2024–T351 and AA7010–T7651) joined by FSW. The effect of the galvanic coupling was investigated using Gel visualization and immersion tests in a 400-mm diameter glass. They found that, the anodic attack was in the AA7010–T7651 alloy with a maximum sensitivity in the nugget zone while for AA2024–T351 alloy the nugget zone was preserved by its high cathodic reactivity as a result of the deposition of S-phase particles.

According to the literature review, few investigations have addressed the optimization of the friction stir welding parameters used in the friction stir lap welding. Moreover, no documentation could be found in the open literature on selecting the friction diffusion cladding parameters of aluminum-alloy (5052-H32)/ASTM 516-70 steel composite layers or the corrosion performance of such layered alloys. Therefore, the purpose of this study is to fill the gaps of the previous work and investigate the fabrication of such cladding using FSDC. This investigation will be conducted based on an experimental work.

# Chapter 3

# Research Methodology

In this chapter research approach, experimental setup, tool design for friction stir diffusion cladding process and tests performed for evaluating the produced joints are presented.

## 3.1 Approach

In the present work, Aluminum alloy sheet was used as cladding material to coat carbon steel substrates to enhance its corrosion resistance and make carbon steel more suited and efficient in a saline corrosive media.

The approach to achieve the research objectives which were mentioned earlier in chapter one is as follows:

1. Selecting grades of aluminum alloy and carbon steel, in addition to defining of process parameters such as: tool rotational and welding speeds, based on published research work.

2. Design and manufacturing of the FSW tool to perform friction stir diffusion cladding process on selected material using defined process parameters.

3. Standard sample preparation processes of cladded samples for standard mechanical, microstructural and corrosion tests.

4. Perform tensile shear and micro-hardness tests to study the effect of the processing conditions on the mechanical properties of the cladded samples.

5. Perform microstructural analysis using optical microscope (OM), scanning electron microscope (SEM), energy dispersive spectroscopy (EDS) and X-ray diffraction (XRD) of the friction stir diffusion cladded samples to investigate the effect of the processing conditions on the formed microstructures and the metallic compounds created between the cladding material and the substrate.

5. Perform corrosion tests including: polarization and impedance tests, considering a standard test solution of 3.5% NaCl to evaluate the corrosion resistance of the produced samples.

## 3.2 Experimental Setup and Procedure

### 3.2.1 Workpiece materials

Aluminum has been reported to have very good corrosion resistance properties in most environments, since aluminium continuously forms a thin but effective oxide layer that stops more oxidation. Aluminium oxide is an impermeable layer and, unlike the oxide layers on many other metals, it adheres strongly to the parent metal. However, if this oxide layer is mechanically damaged, it will repair itself immediately. This oxide layer is considered as one of the main reasons for aluminium's good corrosion properties. The layer is stable in the general pH range of 4 to 9 [41], [48], [50], and [51]. In this study, a 2.0 mm Aluminum alloy (5052-H32) sheet was used for cladding 7 mm thick pressure vessel steel plate ASTM A516-70, because this grade of Al alloy has very good corrosion

resistance, especially in salt-water [16]. The chemical composition and physical properties of the aluminum alloy 5052-H32 and pressure vessel steel A516-70 are listed in Table 1, 2 and 3, respectively. The Al 5052-H32 sheet and the ASTM 516-70 plate were cut into rectangular slab measure 200 mm by 55 mm. This dimension was adopted based on the work of Kimapong and Wantanabe [21] which is suitable for clamping, as well as facilitating the production of subsize tensile-shear test specimen (see figure 3.4). Emery paper was used to clean the mating surfaces of the aluminum (top sheet) and steel sheet (substrate) from any possible oxides or contamination before conducting FSDC. Finally, the surfaces were wiped with acetone [15], [54].

**Table 3.1** Chemical composition and main alloying elements of 5052 Aluminium alloy (weight %) were measured using spark spectroscopy

| Material | Al | Mg | Fe | Si | Cr | Mn | Cu | Ti |
|---|---|---|---|---|---|---|---|---|
| Composition wt.(%) | 96.8 | 2.26 | 0.325 | 0.29 | 0.247 | 0.0863 | 0.0133 | 0.0163 |

**Table 3.2** Chemical composition and main alloying elements of ASTM A516 grade 70 (weight %) were measured using spark spectroscopy

| Material | C | Fe | Si | P | Mn | S |
|---|---|---|---|---|---|---|
| Composition wt.(%) | 0.31 | 97.8 | 0.45 | 0.035 | 1.3 | 0.035 |

**Table 3.3** Mechanical and Physical properties of Al 5052 and ASTM A516-70 steel [55]

| Material properties | 5052 Al alloys | ASTM 516-70 steel |
|---|---|---|
| Tensile Strength Ultimate | 228 MPa | 485 - 620 MPa |
| Tensile Strength Yield | 193 MPa | 260 MPa |
| Modulus of Elasticity | 70.3 GPa | 200 GPa |
| Poissons Ratio | 0.33 | 0.29 |
| Hardness (Vickers) | 68 | 199 |
| Specific Heat Capacity | 0.880 J/g-°C | 0.470 J/g-°C |
| Thermal Conductivity | 138 W/m-K | 52.0 W/m-K |
| Melting point | 607.2 - 649 °C | 1510 °C |

### 3.2.2 FSW machine

FSW machine RM-1; shown in Figure 3.1 a, was used to perform the cladding process, it is computer numerical control (CNC) machine with three degrees of freedom manufactured by MTI. The machine process parameters, in addition to tool reaction loads were recorded by built-in data acquisition system. Position control method was used in the current work, in order to ensure that the machine will maintain a fixed position during the process, not allowing the tool pin to penetrate into the substrate. This method of tool axial control would result in variation of tool axial (forging) force.

### 3.2.3 Clamping system

Similar to FSW, it is very important to have the workpiece rigidly clamped on the backing plate to ensure that the correct process conditions are properly applied. The clamps are used to press the aluminum alloys sheets and the steel substrate against each other to prevent relative movement during the process as shown in figure 3.1 b and c.

(a)

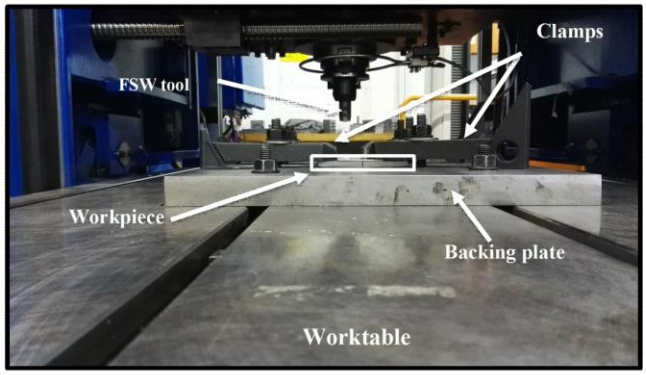


(b)

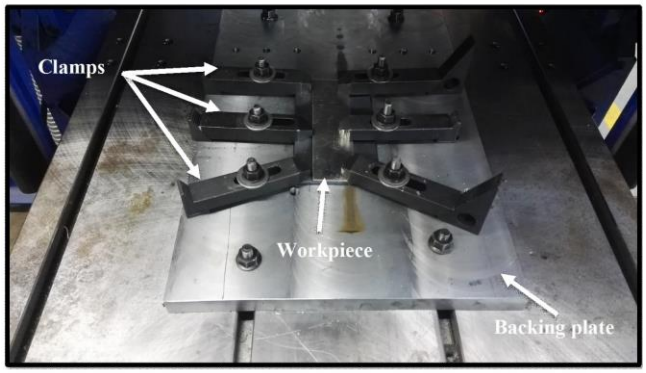


(c)

**Figure 3.1 :** (a) FSW machine RM-1, (b) Clamping system, (c) Clamped sample

### 3.2.4 FSDC Tool Design

The tool has major influence on FSDC process, because the tool controls the flow of material during the process, therefore the tool must be able to bear the mechanical and thermal stresses developed during the process. The tool consists of two components, a shoulder with two circular groves on its bottom surface to enhance the material flow of 23 mm diameter, and non-threaded cylindrical tool pin with a diameter of 7.5 mm (the most commonly used ratio of shoulder-to-pin diameter is 3 [56]), and an adjustable pin length as shown in figure 3.2. Since the clad material is soft (5052-H32 aluminum alloy), tool steel grade 4140 was selected as FSDC tool body (shoulder) whereas AISI H13 tool steel was used for manufacturing the pin.

The manufactured tool was then heat treated to increase the hardness of the tool to a range of 52-55 HRC. The heat treatment was performed according to the following steps:

1. Preheated for 30 minutes at 200 $^{o}$C to avoid thermal shock.
2. Then, the furnace temperature was increased rapidly to 850 $^{o}$ C and the tool was kept at this temperature for 30 minutes.
3. After that to increase the hardness, tool shoulder was quenched in water while tool pin was left to cool down at room temperature.
4. Then both were tempered at 200 C$^{o}$ for 20 minutes to retain some ductility.

The average value of hardness was calculated from 6 measurements and it was found to be 55 HRC for tool shoulder and 58 RC for the tool pin.

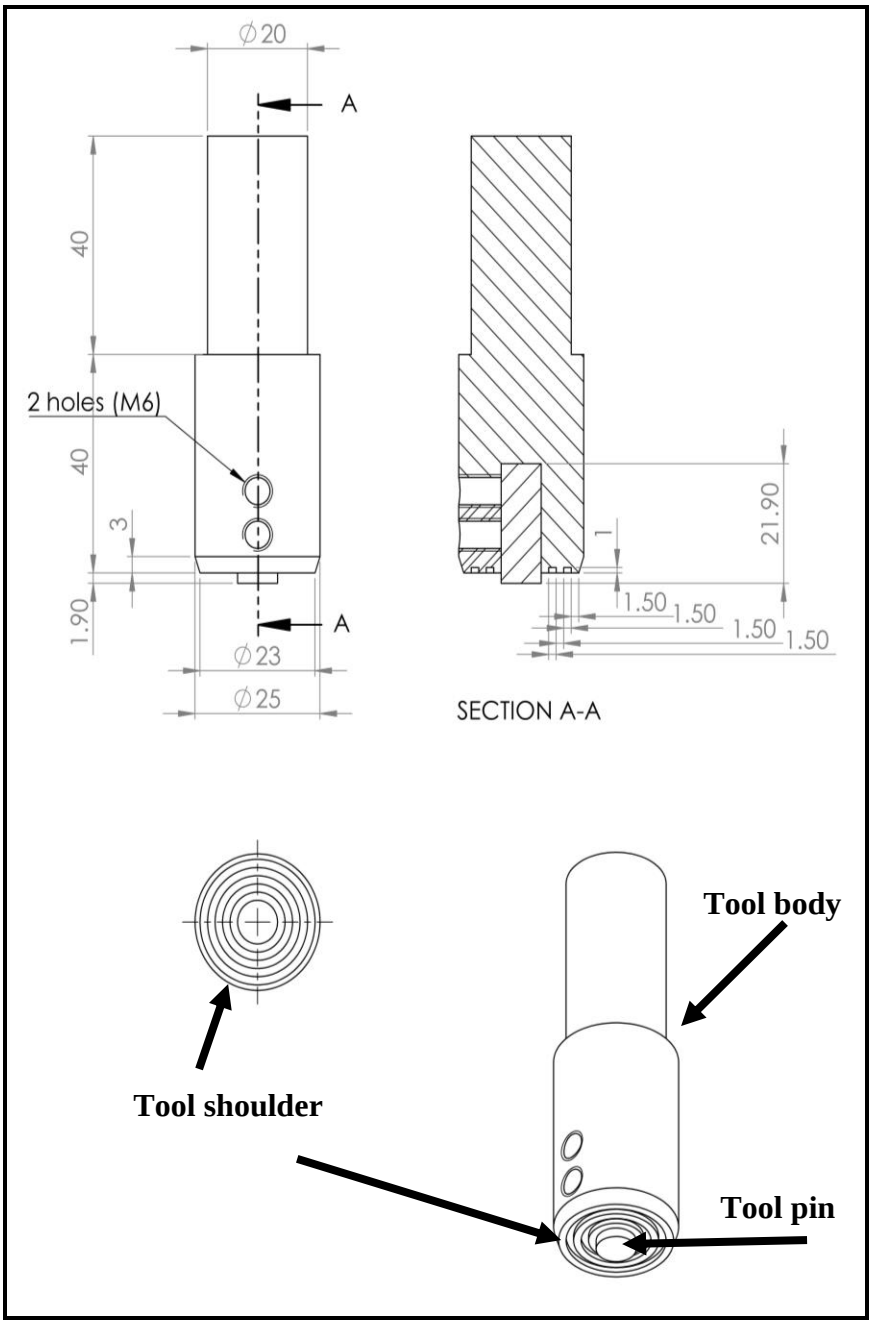


**Figure 3.2:** FSDC tool body, tool pin and shoulder. (All dimensions are provided in mm)

### 3.2.5 Process parameters

The specified process parameters from the literature review [21], [29] were useful but may not be effective to identify the best process parameters that give the maximum joint strength, and corrosion resistance for the selected material, due to the differences in workpiece thickness, materials (substrate and clad), and tool geometry. Since inadequate data was published about the best process parameters, an experimental matrix was developed to investigate the effect of rotational and travel speeds on joint strength. The tool tilt angle was set to zero degree to avoid any constraint in the welding direction. In addition, it has been reported that increasing the tilt angle will increase the thickness of the IMCs layer which will affect the joint strength significantly [29]. Nine sets of process conditions were adopted to study the effect of process parameters i.e. tool rotational speed and travel speed on joint strength as well as corrosion resistance, as listed in Table 3.4.

**Table 3.4** Experimental Matrix

| **Travel speed (mm/min)** | **Rotation Speed (rpm)** | | |
|---|---|---|---|
| | **1000** | **500** | **250** |
| **50** | A50 | B50 | C50 |
| **100** | A100 | B100 | C100 |
| **150** | A150 | B150 | C150 |

## 3.3 Characterization of cladded samples

After cladding process took place, the produced samples were sectioned to generate specimens for tensile-shear test, and corrosion, while mounted, grinded, polished and etched using 2% Nital etchant (a mix of ethanol and Nitric Acid) for few seconds until the color changes for metallographic, SEM, and XRD tests.

Mechanical tests (tensile shear, and microhardness) were carried out using Instron universal tensile test machine with maximum capacity of 100 kN (figure 3.3), and microindentation hardness tester (MicroCombi, CSM Instruments, Switzerland) was used to measure hardness at the interface, heat affected zones and base material respectively. These tests were performed to study the effect of process parameters on strength of the clad joint, as well as the variation in microhardness at the joint interface. For tensile shear tests, the cladded samples were cut according to the standard sub size samples reported by [25] as shown in figure 3.4. Spacers were attached to tensile-shear test samples (see figure) to properly align the specimen with the machine Jaws during the test and to avoid presence of eccentric loading on the joint, ensuring pure shear load on the lap joint during the test. The tests were conducted at a ram speed rate of 2 mm/min [25]. Similarly, for the microhardness test 0.1 N load was applied, with 10-second dwell time.

Microstructural analysis was used to reveal material structural changes that occurred by FSDC process. This helped to identify the effect of process parameter on aluminum and steel structures, and diffusion layer by looking into its; thickness, profile geometry, or any other microstructural changes. Metallography was performed using optical microscope and macro-imaging camera to study both micro- and macrostructures of the weld joint, as well as the metallurgical bond geometry. SEM was used for imaging while XRD was used to identify the phases on the cross section of the joint interface. Also, Energy Dispersive spectroscopy (EDS) along with mapping analysis were implemented at several locations of the joint interface to detect the elemental diffusion of aluminum into steel and vice versa. A Starrett R200 stylus Profilometer was used to measure the surface

roughness of the processed samples to help understanding the corrosion performance of the different cladded samples.

### 3.4 Corrosion Testing

Electrochemical data were collected using a potentiostatic–galvanostatic GAMRY600 corrosion measurement system (GAMRY, USA). The electrochemical cell used for the Tafel polarization study consisted of the cladded steel sample as the working electrode, a graphite rod as the counter electrode, a standard calomel electrode (SCE) as the reference electrode, and 3.5 wt.% aqueous sodium chloride solution as the electrolyte as shown in figure 3.5. NaCl solution (3.5 wt.%) was selected for testing the corrosion behavior because it is the typical salt concentration in seawater, therefore if we tested the sample at 3.5% NaCl it is possible to report against the most common corrosive agents.

Electrochemical surface masks with a circular area of 1 $cm^2$ were used to locate a specific area for electrochemical analysis. For Tafel polarization measurements, the potential was scanned from -0.25 V to 0.25 V with respect to the open circuit potential (OCP) at a potential scanning rate of 1 mV/s. The protective behavior against corrosion was also studied by conducting electrochemical impedance analysis, and data were collected using a GAMRY600 potentiostat with a frequency range between 100 kHz and 10 mHz. The number of points taken was 10/decade with an AC voltage of 10 mV. Data fitting and electrochemical simulations were carried out using the E-Chem Analyst software.

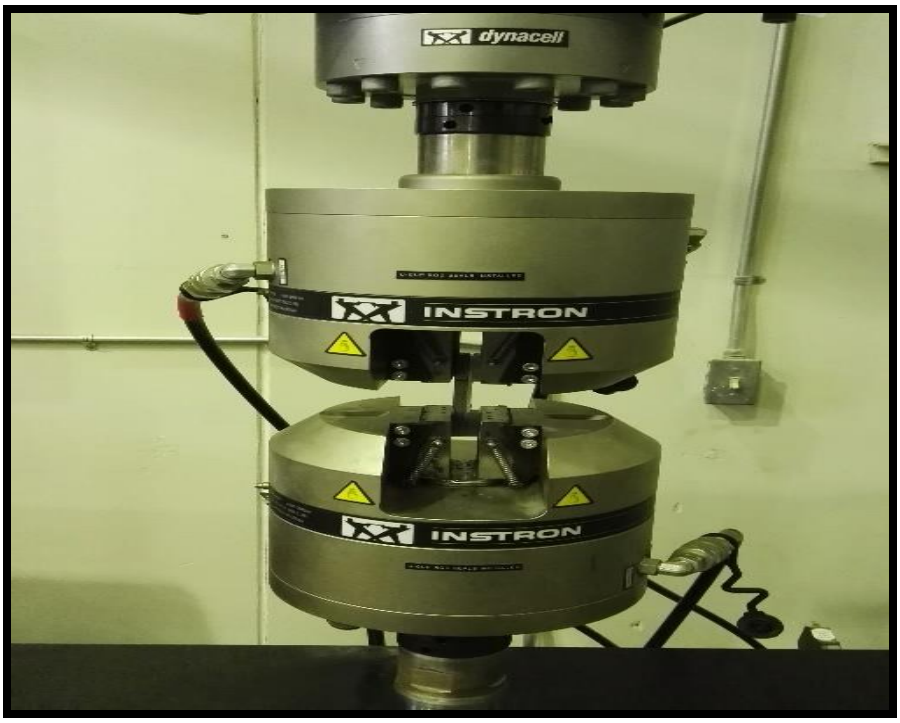


**Figure 3.3: Tensile test machine**

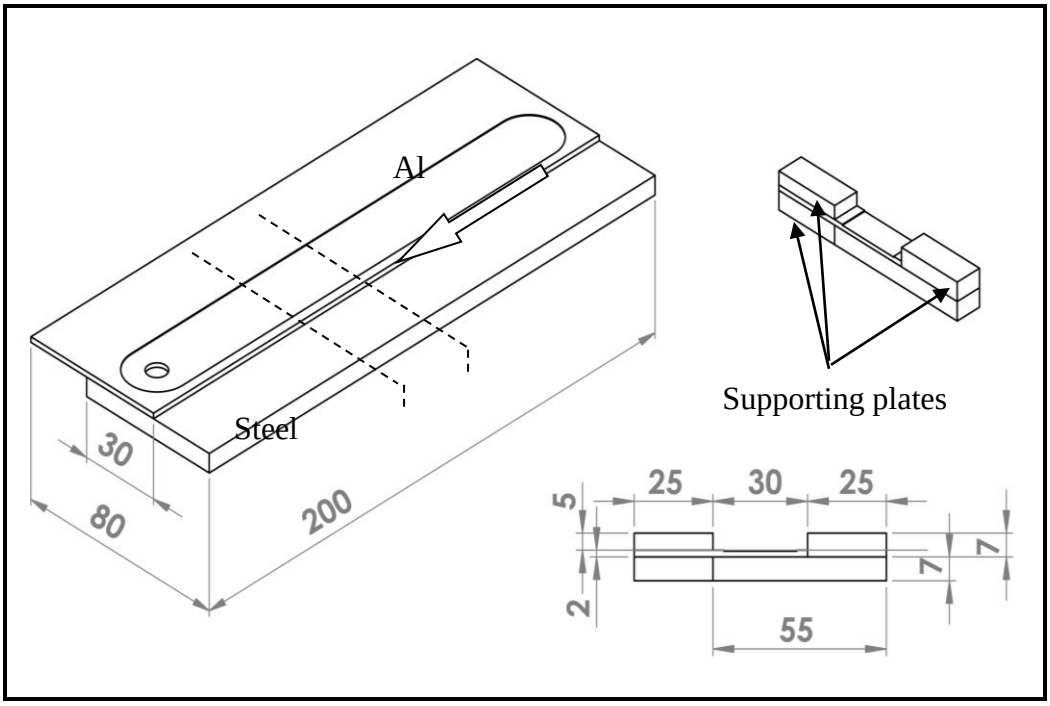


**Figure 3.4: lap joint schematic and tensile shear specimen (dimensions in mm).**

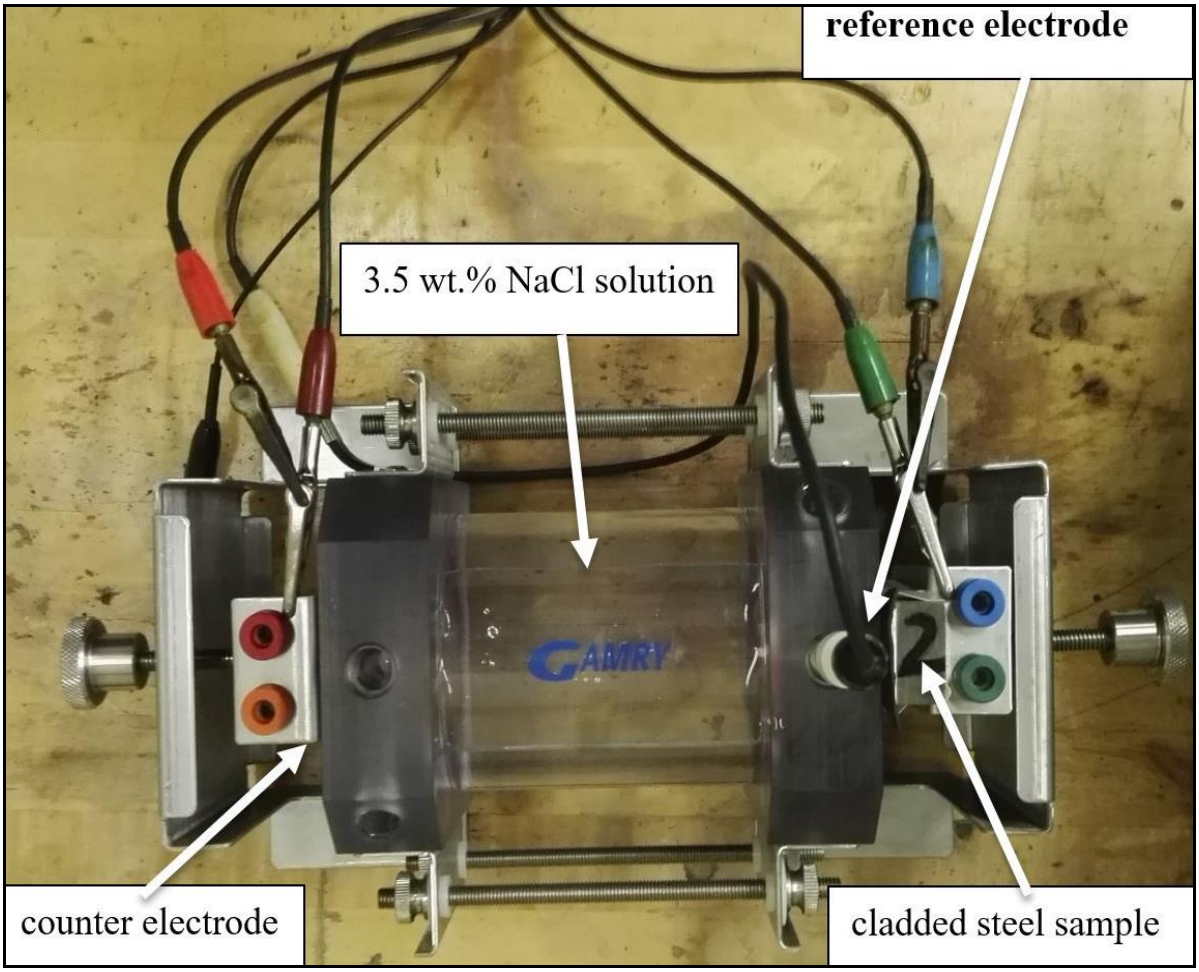


**Figure 3.5:** Electrochemical cell and corrosion test setup

# Chapter 4

# Results and Discussion

In this chapter results obtained from the experimental works and tests performed for evaluating the joint will be presented and discussed.

## 4.1 Surface morphology

### 4.1.1 The effect of process parameters on surface quality

As shown in Table 4.1, FSDC process was successfully achieved at the listed process conditions. Most of the samples were well bonded except for C100 and C150 which had very weak bonds as the clad sheets were easily detached from the substrate after the process. This can be due to the low heat input produced at such process parameters; low rotational speed (250 rpm) and high travel speed (100 and 150 mm/min). Moreover, at the rotational speed of 1000 rpm, samples A100 and A150 had some surface defects including voids and lack of fill, while sample A50 was found defect free, as shown in figure 4.1. These defects were attributed to the high strain rate generated at high welding speed as well as fluctuation of dynamic load and vibration during the process as shown in figure 4.2. The imperfect bead appearance was also reported by [22], and the author identified the issue to the application of zero tilt angle.

Photographs of samples produced (attached to table 4.1) show the effect of process parameters on surface conditions; i.e. surface roughness, flash and surfaces defects if any. It was clear that, all cladded samples had flat surface with the presence of flash at the retreating side along the processed area. Also, the formation of keyhole at the end of the process after retracting the FSDC tool. There was no sign of distortion on the FSDC samples, due to higher thickness (7mm) of the ASTM 516-70 steel plate which increases the amount of heat dissipation during the process.

Alternatively, all samples had showed a uniform roughness from the beginning to the end of the bead. A Starrett R200 stylus Profilometer was used to measure the surface roughness of the processed samples, as shown in figures 4.3 (a)-(c). From profilometer measurements, it has been noticed that at constant travel speed, as the rotational speed increases the surface roughness decreases; for instance, sample A50 has smoother surface roughness compared to B50 and C50. In contrast, at constant rotational speed as the travel speed increases the surface roughness increases too, as for samples B50 have smother bead surface than B100 and B150 respectively, see Table (4.2).

The surface roughness can be identified by the tool advance per revelation (APR) which defined as the ratio of the applied travel to rotational speeds during the process. As this ratio increases the surface roughness increases too and vice versa. For instance, at constant rotational speed of 1000 rpm and 50mm/min travel speed the APR is 0.05 mm/ revelation, while the APR is 0.1 mm/ revelation when 100 mm/min was applied.

**Table 4.1:** Top view of FSDC samples at different welding and rotational speeds.

| Sample | Process parameters | Bead |
|---|---|---|
| A50 | N = 1000 RPM<br>V = 50 mm/min<br>PD = 2 mm<br>N/V = 20 | 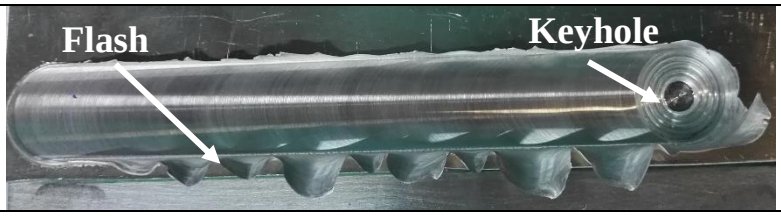 |
| A100 | N = 1000 RPM<br>V = 100 mm/min<br>PD = 2 mm<br>N/V = 10 | 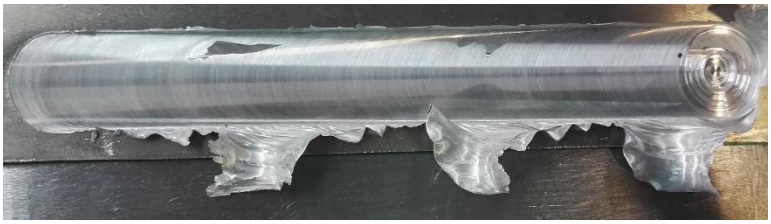 |
| A150 | N = 1000 RPM<br>V = 150 mm/min<br>PD = 2 mm<br>N/V = 6.667 | 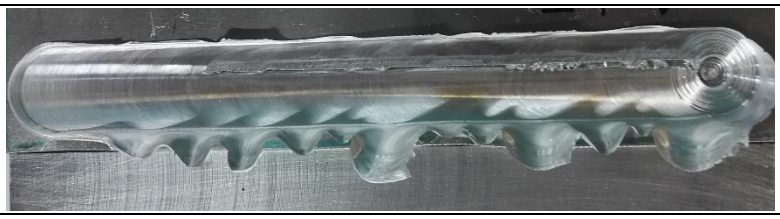 |
| B50 | N = 500 RPM<br>V = 50 mm/min<br>PD = 2 mm<br>N/V = 10 | 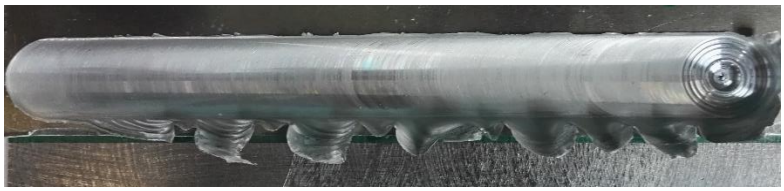 |
| B100 | N = 500 RPM<br>V = 100 mm/min<br>PD = 2 mm<br>N/V = 5 | 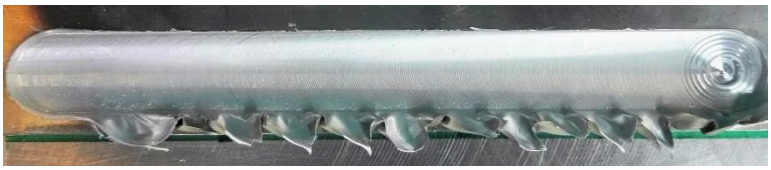 |
| B150 | N = 500 RPM<br>V = 150 mm/min<br>PD = 2 mm<br>N/V = 3.333 | 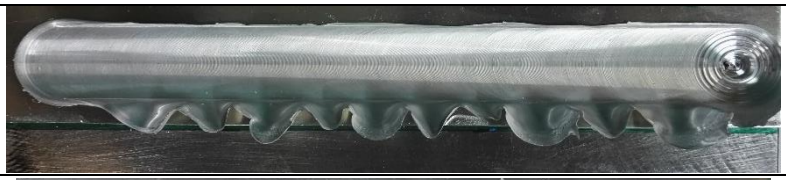 |
| C50 | N = 250 RPM<br>V = 50 mm/min<br>PD = 2 mm<br>N/V = 5 | 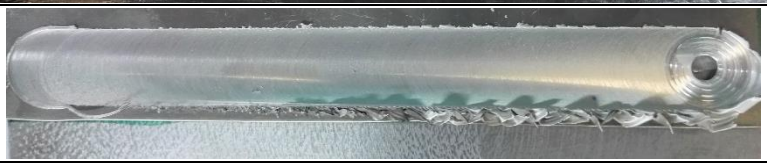 |

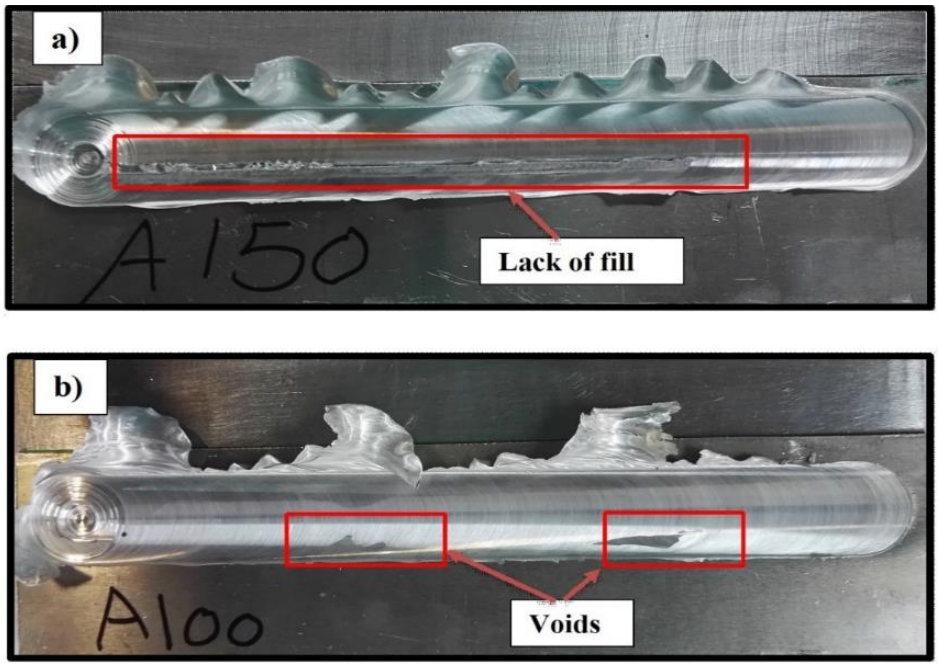


**Figure 4.1:** Surface defects of FSDC samples a) Lack of fill at sample A100, b) Voids formed at sample A 150

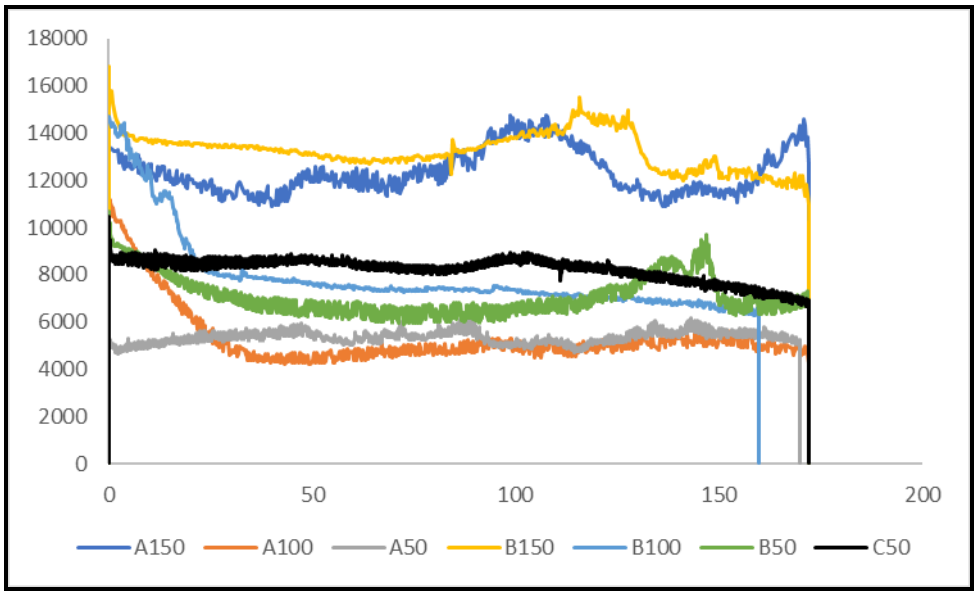


**Figure 4.2**: Axial Force at different FSDC process conditions.

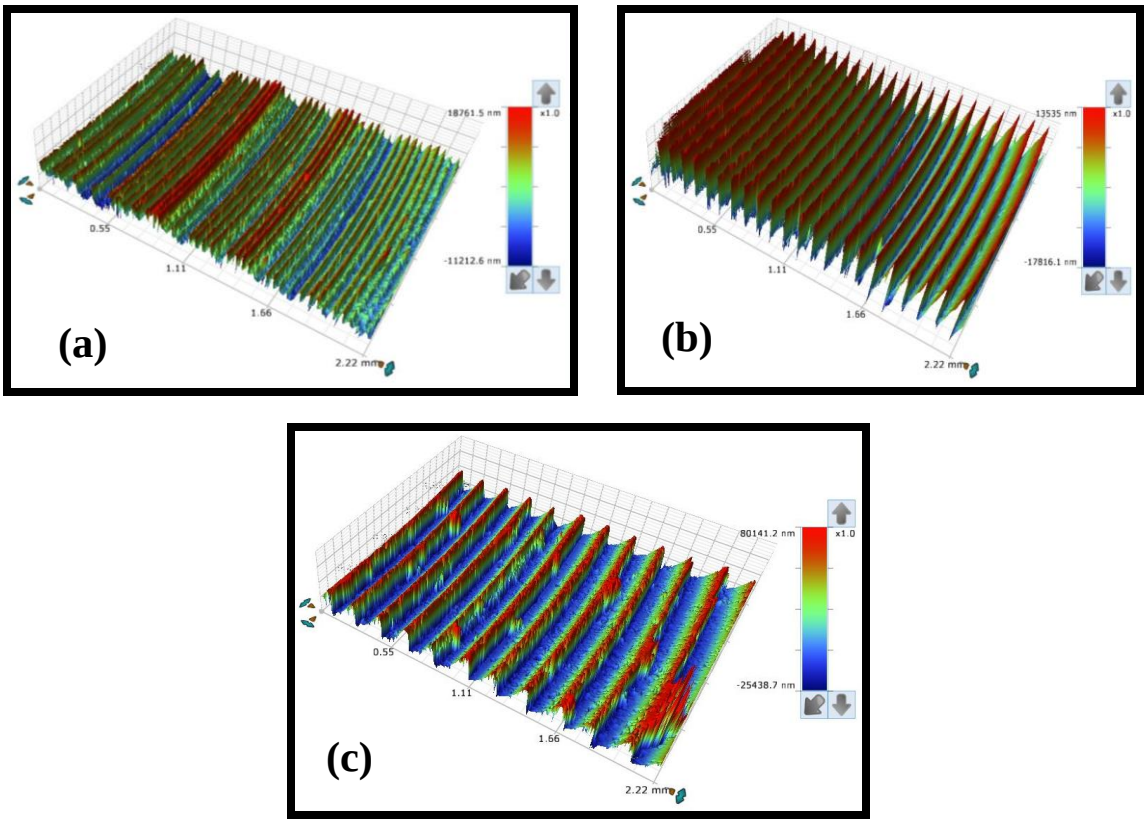


**Figure 4.3**: Surface roughness of cladded samples at 50 mm/ min welding speed and different rotational speed of a) 1000 b), 500, c) 250 (RPM)

**Table 4.2:** Surface Roughness measurements for the FSDC samples

| Average value | **$R_a$** (µm) | **$R_{sm}$** (µm) | **$R_z$ (µm)** |
|---|---|---|---|
| A50 | 2.240286 | 2.647516 | 11.212594 |
| B50 | 5.150444 | 5.941616 | 17.816148 |
| C50 | 10.266459 | 11.870151 | 25.438684 |

Where:

**$R_a$** is the arithmetic mean for height parameter.

**$R_z$** is the profile's maximum peak to valley height equivalent to the sum of the maximum peak height and the maximum valley depth.

**$R_{sm}$** is the average distance between profiles peaks at the mean line.

## 4.2 Microstructural and Materials characterization results

### 4.2.1 Optical Microscope (OM)

The cross section of cladded samples was characterized by optical microscope (OM) and scanning electron microscope (SEM) to reveal microstructure details, bonding thickness and continuities of the joint, as well as to compare their microstructure with the base material. All defect free cladded samples were sectioned perpendicular to tool travel direction, grinded, polished and etched. The aluminum sheet used for cladding was produced by cold rolling process, which made it difficult to identify the aluminum grains. However, it was only possible to reveal the grains at the steel side. The micrographs of as received A516-70 steel showed ferrite and pearlite microstructure; as presented in figure 4.4. Due to FSDC process; as shown in figure 4.5, it can be noticed that A516-70 steel grains were refined near the interface, and grow away from it. This had occurred due to recrystallization of steel grains as it is subjected to heat and pressure resulted in sever plastic deformation. Mechanical mixing of clad material with the substrate was found at the joint interface under the pin, when high rotational speed of 1000 rpm was used along with 50 mm/min travel speed as presented in figure 4.5. At such conditions, the heat input was high enough to soften the clad material and make it easy to flow and mechanically mix with the substrate, therefore the softened material was pushed to diffuse into the base material by the forging effect.

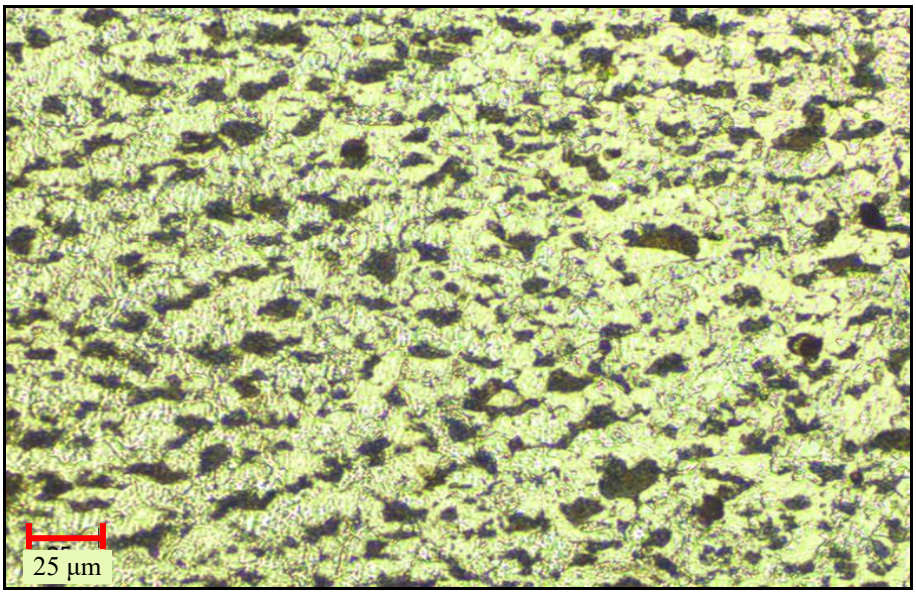


**Figure 4.4**: Optical microscope image of ASTM A516-70 base material

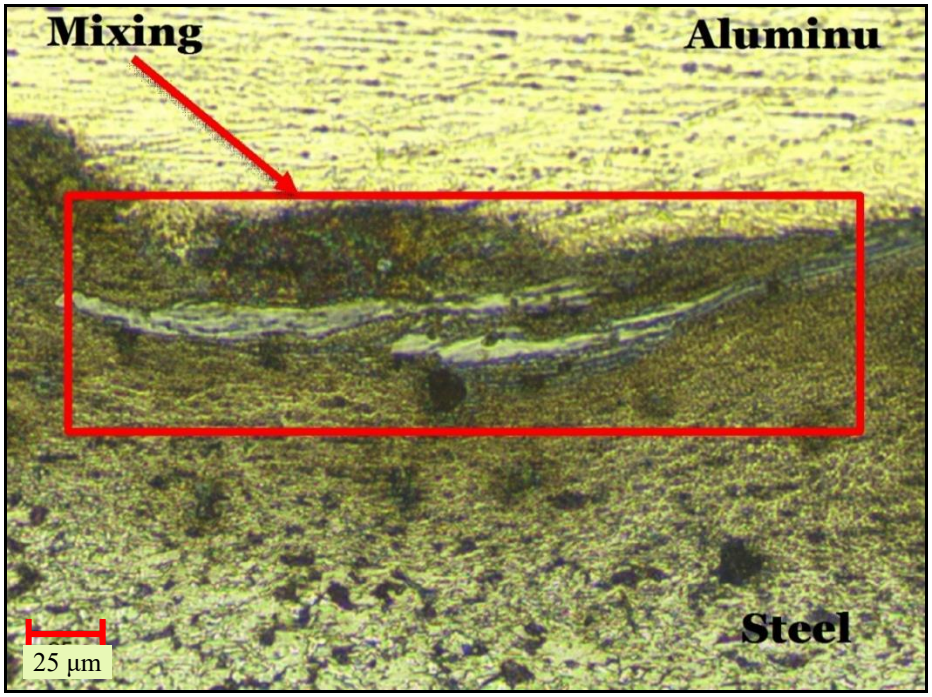


**Figure 4.5 :** Mechanical mixing of clad Aluminum and Steel at 1000 RPM and 50mm/min

The effect of rotational and travel speeds on the microstructure was investigated. For a fixed tool travel speed, the grain size increased with increasing the tool rotational speed; this was expected due to the increasing of the frictional heat, therefor grains growth will take place, this result was strongly agree with the previous results reported by [23], [57], [58].

However, it was not possible to see any grains closed to the joint interface of all cladded samples compared with the other zones, because of the compression produced by the applied forging force as well as the heat generated and plastic deformation between the tool pin and workpiece as seen in figure 4.9. It was only possible to see them near the heat affected zone (HAZ). Two types of steel structure were detected at all process parameters, pearlite which is lamellar layered structure and ferrite as shown in figure 4.3.

Table 4.3 summarize the average grain size of steel at fixed travel speed of 50 mm/min and different rotational speeds, the grain size was measured by FESEM and the average value was calculated using excel sheet and by another software called (image J). The average grain size is listed on table 4.3.

In contrast, at constant rotational speed as the travel speed increases the grain size decreases due to the lower heat input as shown in Figure 4.10. This results strongly agrees with those of previous articles [23], [57], [58]. The average grain size at different welding speeds was listed in Table 4.4.

**Table 4.3:** The average grain size of steel at different rotational speeds (rpm)

| Sample | A50 | B50 | C50 | Base steel |
|---|---|---|---|---|
| Average grain size (µm) | 48.605 | 41.75 | 40.8075 | 38.7 |

**Table 4.4:** The average grain size at different travel speeds (mm/min)

| Sample | A50 | A100 | A150 |
|---|---|---|---|
| Average grain size (µm) | 48.605 | 46.68 | 42.5175 |

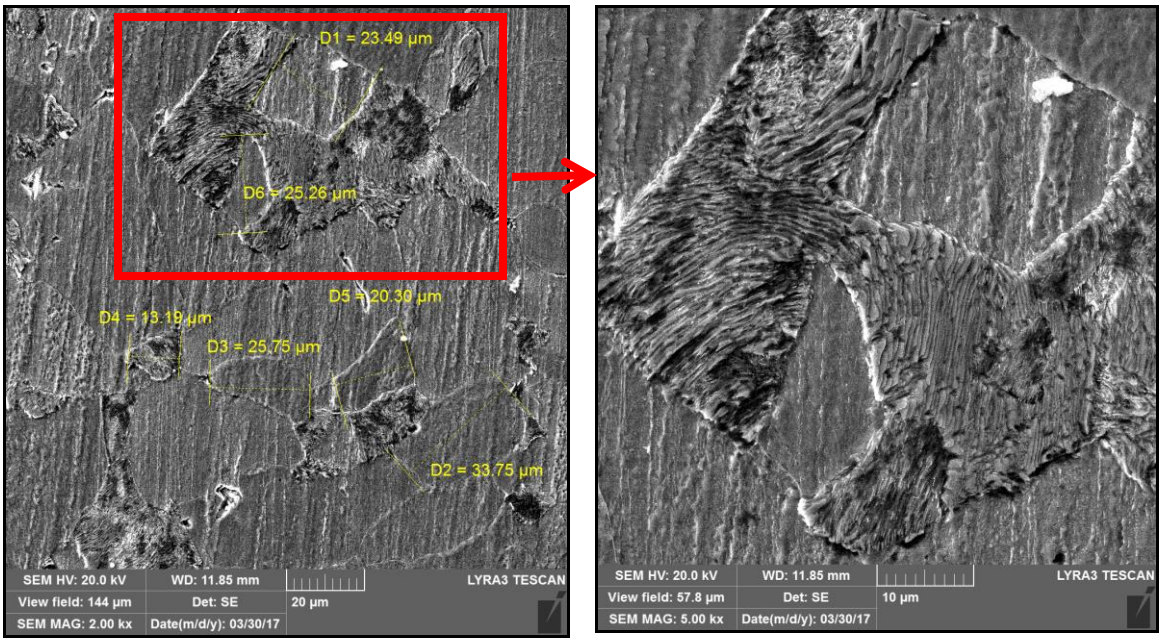


**Figure 4.6:** Pearlite lamellar (layered) structure at 1000 RPM and 50mm/min.

### 4.2.2 SEM and EDS analysis

SEM and EDS were used to further study the developed interface between the aluminum and steel and determine the developed grain size. The SEM images of all cladded samples were captured using back scattered electron mode. Several defects as cracks and voids were detected at the interface of sample A50 and B100 (Figure 4.7 (a), and (e)), which could be due to the high heat input. Since Aluminum and steel have different thermal expansion and heat capacitance, after the process is done, the rapped cooling in Aluminum compared to steel resulted in higher contraction in aluminum therefore fracturing the week bonding zones. On the other hand, lack of consolidation in sample C50 and B150 was attributed to the lower heat input, as can be seen from Figure 4.7 (f) and (g) respectively. The interface of sample B50 (Figure 4.7 (d)) was found to be defect free with good metallic bonding between the clad material and the substrate.

EDS analysis was used to identify the chemical composition (elemental analysis) at selected regions using area analysis, line scan technique. EDS line scan analysis was conducted at the cross section of the clad joint to detect the diffusion and distribution of the elements at the interface as shown in figure 4.8. The thickness of the diffusion layer at the interface of the cladded samples were listed in table 4.5, the maximum thickness of the intermetallic layer formed at the interface was measured by EDS line scan and it was found to be about 4.5 µm when 500 RPM and 50 mm/min was applied as shown in figure 4.8. Therefore, to identify these phases X-ray diffraction was used as shown in figure 4.11.

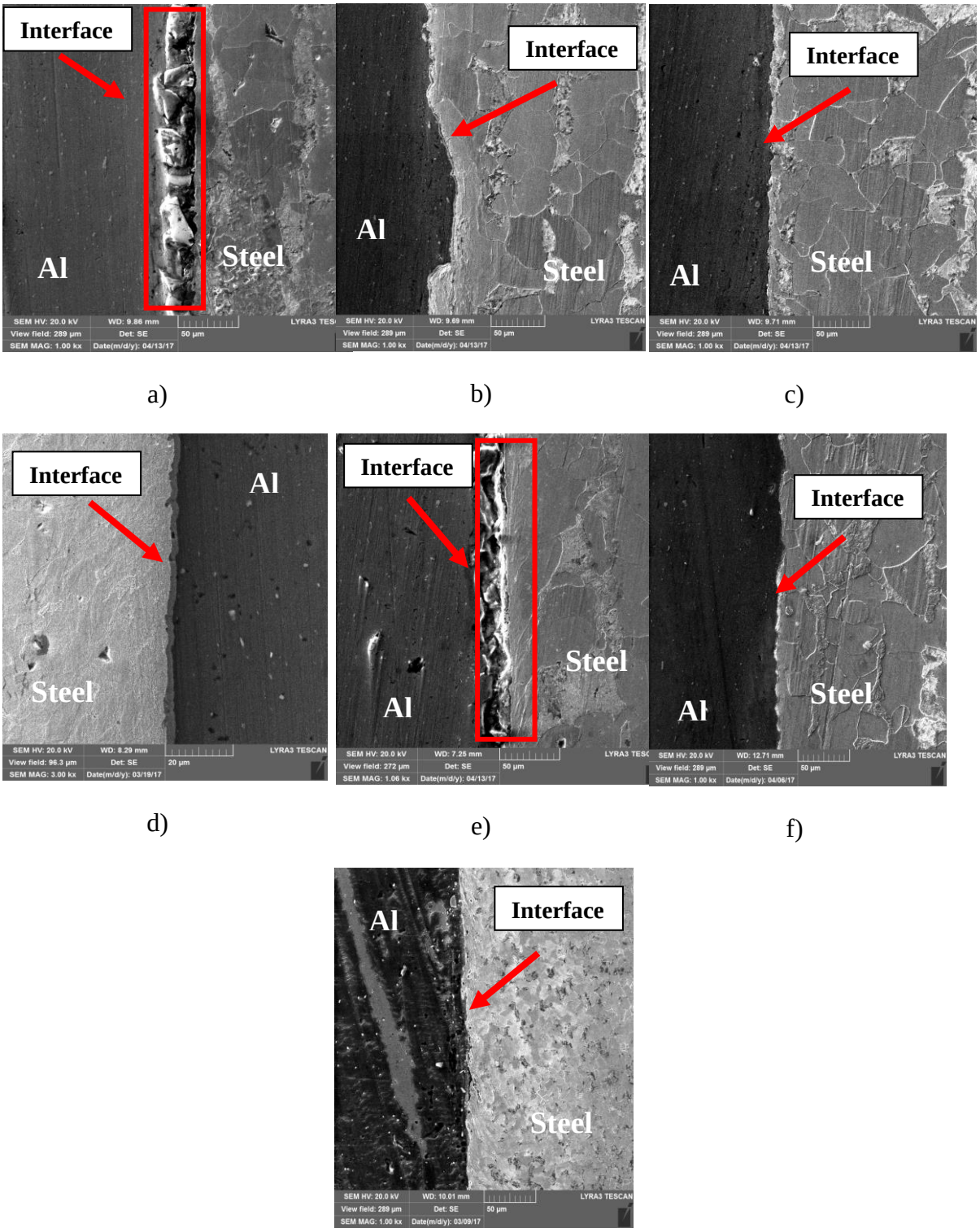


**Figure 4.7:** SEM images of all cladded samples at interface a) A50, b) A100, c) A150, d) B50, e) B100, f) B150 and g) C50.

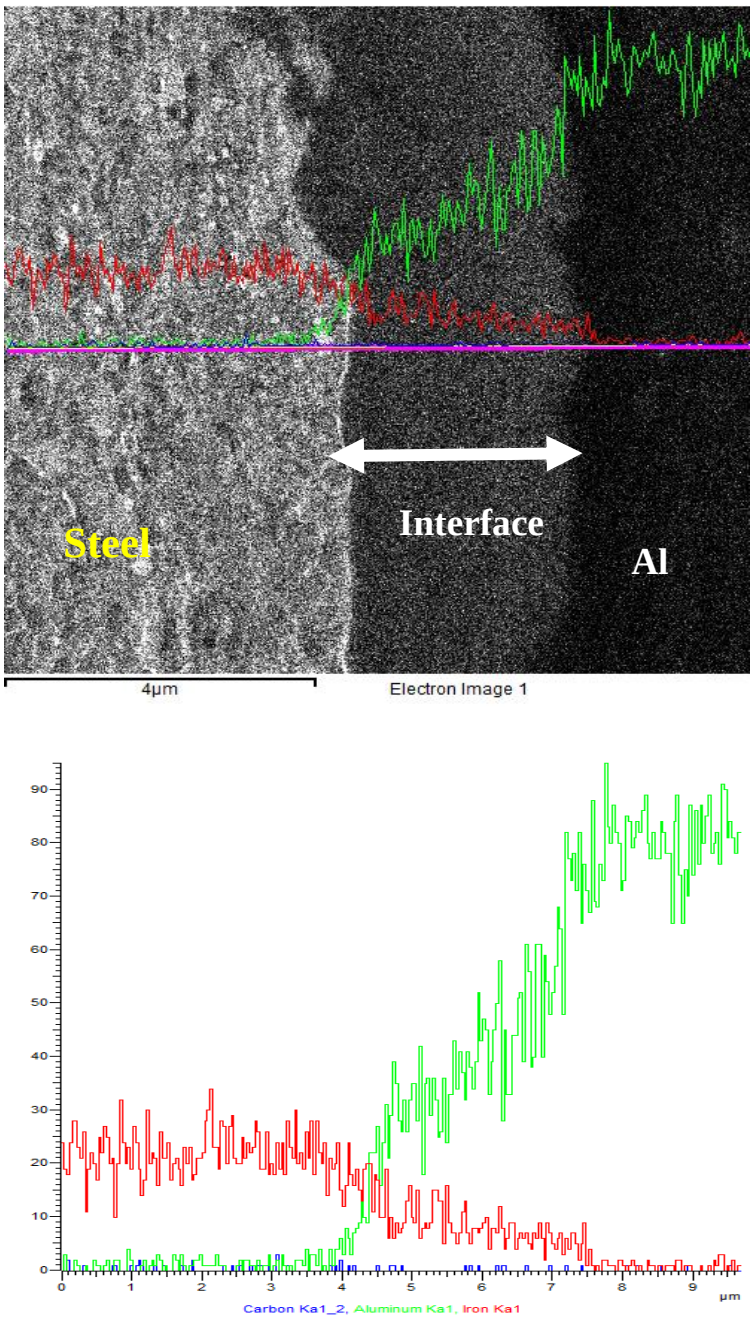


**Figure 4.8:** EDS analysis - line scan of sample B50.

**Table 4.5:** The thickness of the diffusion layer at the joint interface

| **Sample** | **A50** | **A100** | **A150** | **B50** | **B100** | **B150** | **C50** |
|---|---|---|---|---|---|---|---|
| Thickness of the diffusion layer **(µm)** | 7 | 3 | 2.5 | 4.5 | 4 | 2.7 | 2 |

### 4.2.3 XRD results and analysis

X-ray diffraction data were used to identify the intermetallic compounds formed at the joint interface. As can be seen from XRD patterns, Al, Fe and an intermetallic compound of $Al_{13}Fe_4$ were detected in all the tested samples. The same intermetallic phase ($Al_{13}Fe_4$) was also reported by [15], [18], [23], and [24] in addition to some other phases such as $Fe_2Al_5$ and FeAl, they have suggested that these IMCs are responsible for the brittle fracture of the joints at lower loads. However, they have recommended to control the process parameters like; pin depth, rotational and travel speeds, and tool tilt angle in order to reduce the thickness of the intermetallic compounds and enhance the joint quality between Al and steel.

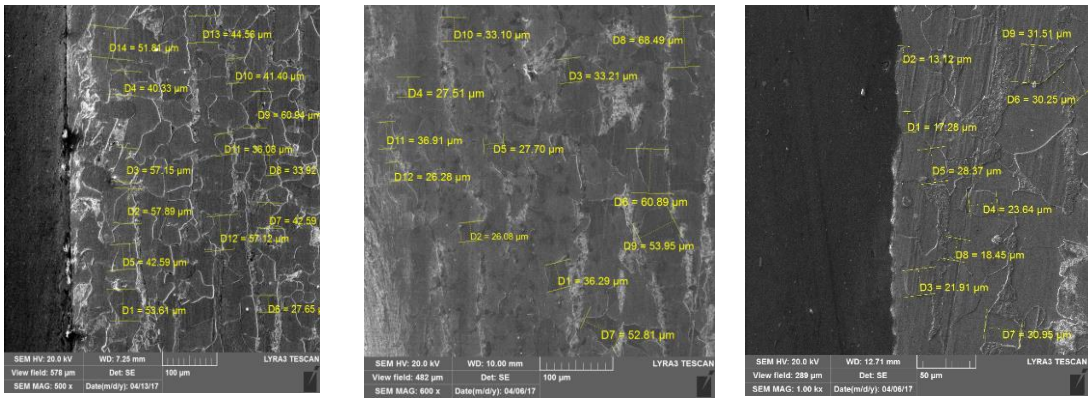


a) b) c)

**Figure 4.9: SEM images reveal the effect of rotational speed on steel grain size at fixed welding speed of 50 mm/min and a) 1000 rpm, b) 500 rpm, and c) 250 rpm**

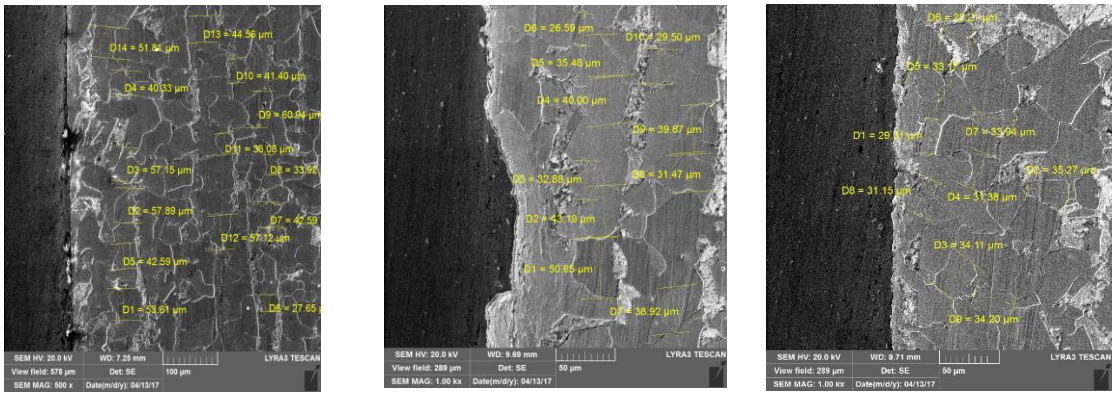


a) b) c)

**Figure 4.10: SEM images reveal the effect of welding speed on steel grain size at fix rotational speed of 1000 and a) 50 mm/min, b) 100 mm/min, c) 150 mm/min.**

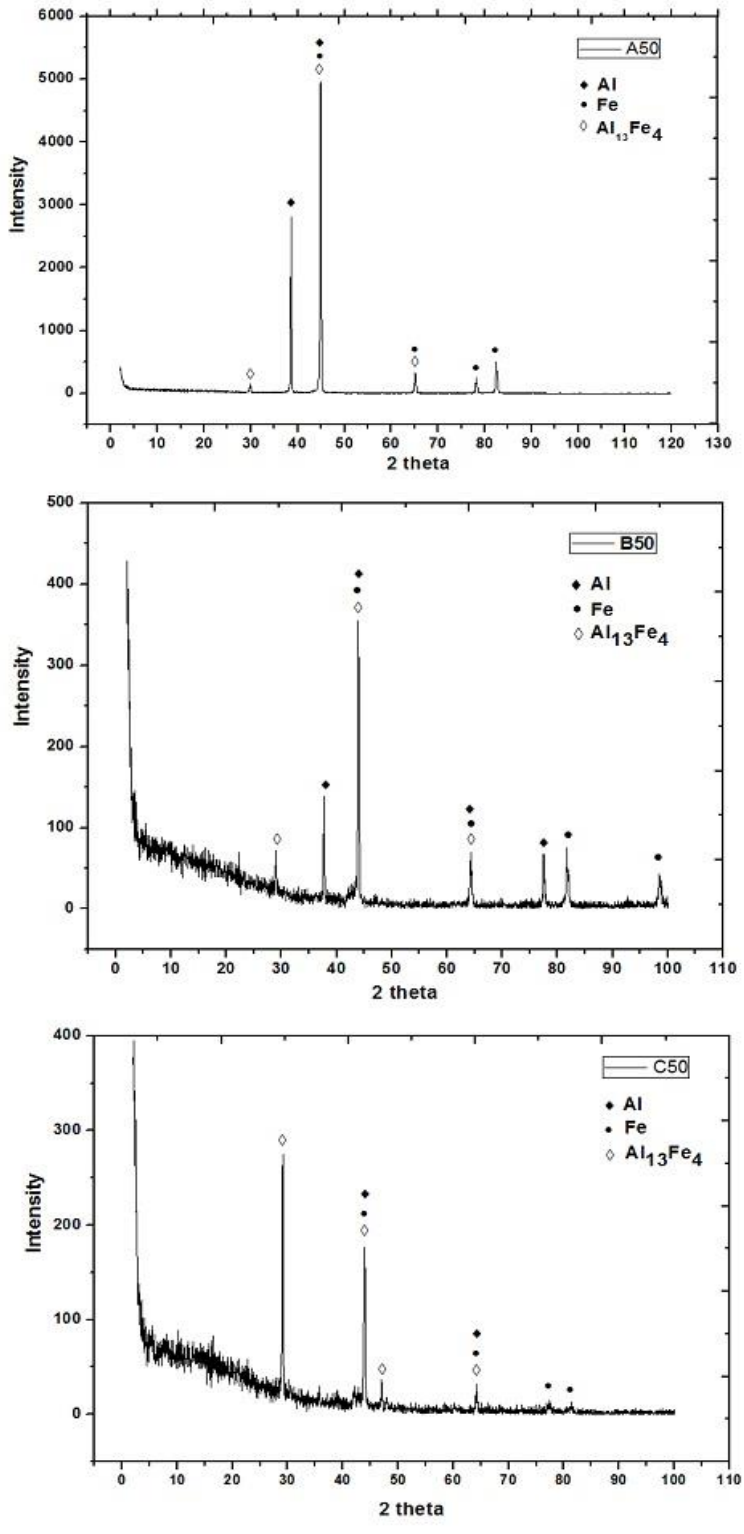
A50
Al
Fe
Al13Fe4
Intensity
2 theta
B50
Al
Fe
Al13Fe4
Intensity
2 theta
C50
Al
Fe
Al13Fe4
Intensity
2 theta

a)

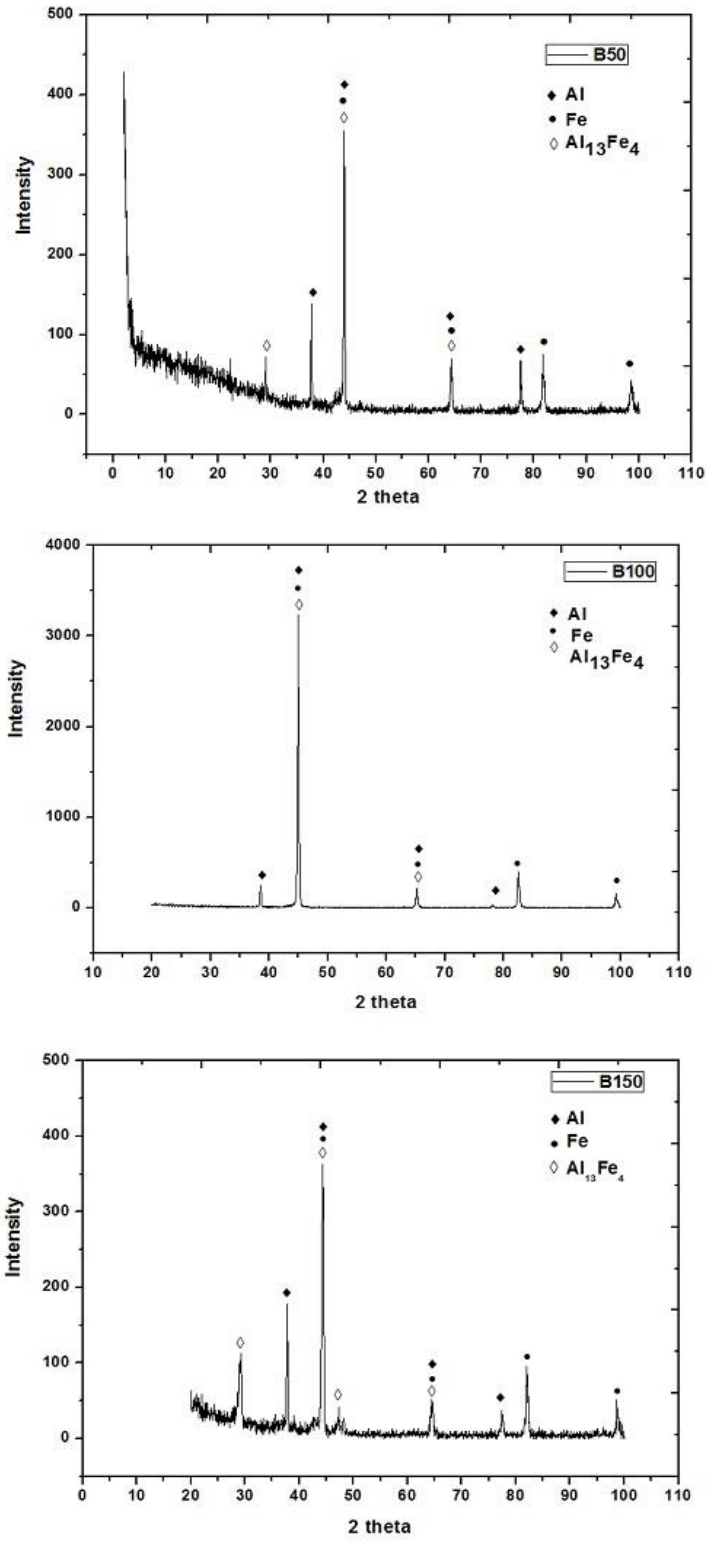


b)

**Figure 4.11:** Shows the XRD patterns of the interface for all cladded samples and the diffraction lines for Al, Fe, and $Al_{13}Fe_4$ phase.

## 4.3 Mechanical tests results and discussion

### 4.3.1 Microhardness

Vickers's microhardness measurements were performed across the interface between Aluminum and steel, heat affected zone and the base metals. The applied load was set to 300-gram force (gf), with 10-second dwell time. Five indentations were performed to identify the average hardness at the middle of the process zone, below the FSDC tool pin; as can be seen from figure 4.12 for sample A50. The average hardness values are summarized for each column at both materials and the interface as shown in Table 4.5; moreover, hardness profile along the cross section is plotted as shown in figure 4.13. The maximum hardness value was recorded at sample A50, because of the sever plastic deformation.

The hardness at interface was higher than the base materials, because of grain refinement as well as the formation of IMCs phases. The hardness value was found to be reducing as away from the interface. In aluminum side, mechanical deformation caused by the FSDC tool pin as well as the forging force resulted in increasing its hardness to 124.062 HV which was higher than that of the base material (68 HV).

The hardness profile at the joint interface shows an average hardness value of 429.089 HV which was two times greater the hardness at steel base material (200 HV). As the rotation speed increases the hardness value at the interface increases too, this was attributed to the high heat generated by friction at high rotational speed between the FSDC tool and the workpiece, as a result of high heat input hard IMCs phases will be formed. while increasing the travel speed will reduce the heat input therefore less IMCs will be formed and the hardness will decrease at the interface.

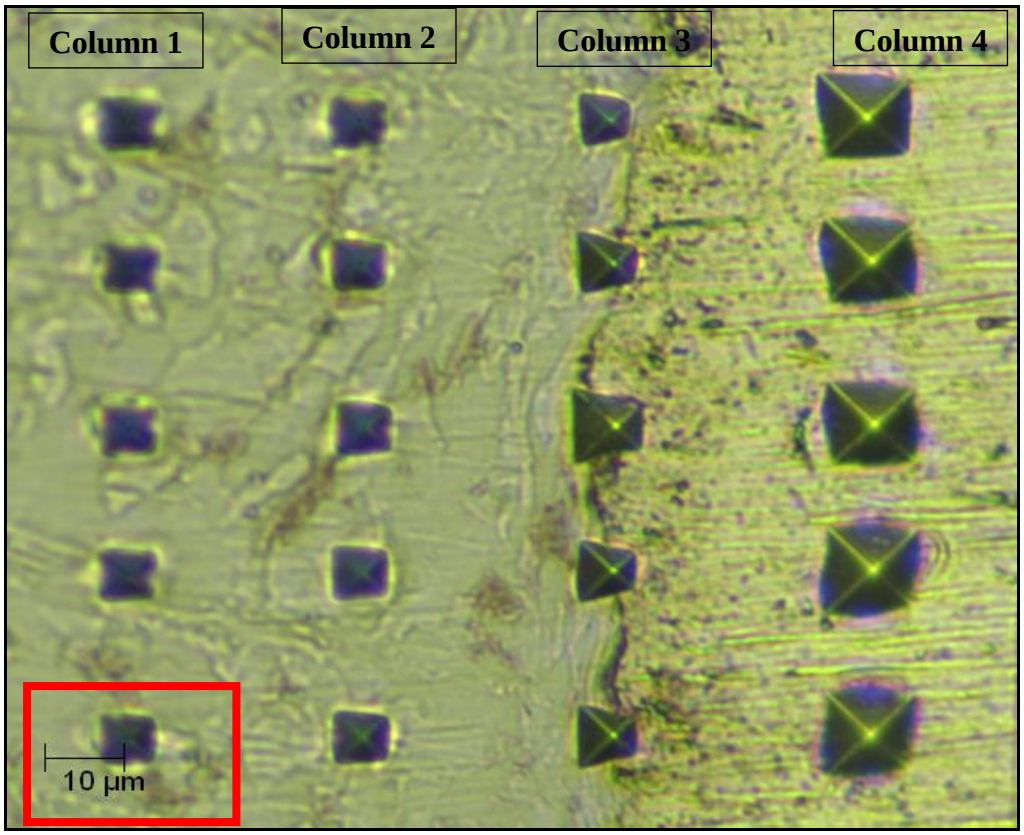


**Figure 4.12:** Hardness distribution along the cross section of the clad sample A50.

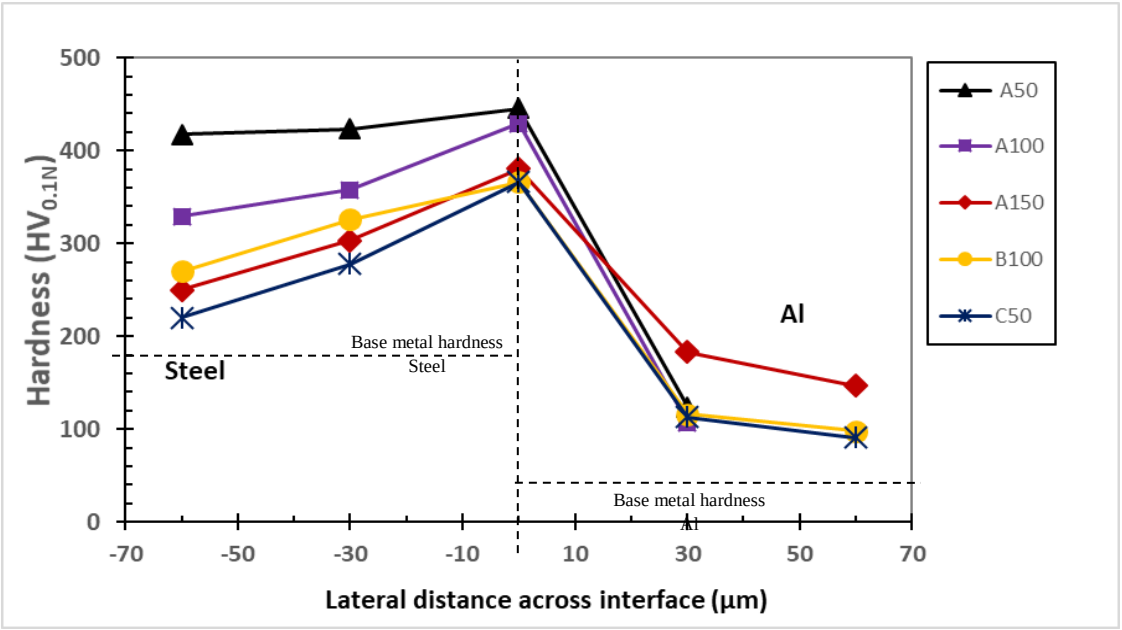


**Figure 4.13 :** Hardness profile along the cladded sample cross section

**Table 4.6** : Average Hardness values at the cross section of a cladded sample.

| Column number | Average Hardness value | |
|---|---|---|
| | MPa | Vickers (HV) |
| **1 (steel)** | 4423.398 | 417.507 |
| **2 (steel)** | 4485.073 | 423.328 |
| **3 (interface)** | 4546.112 | 429.089 |
| **4 (aluminum)** | 1314.415 | 124.062 |

### 4.3.2 Tensile-shear strength

Lap joint configuration was used to evaluate the shear strength of the clad samples. Three test coupons were cut from each sample as shown in Figure 4.14, and grinded to smoothing the surface and remove the sharp edges which may act as stress rises. During sample preparation, joints C100 and C150 failed, therefore they were excluded from tensile shear tests.

At 1000 rpm rotational speed, the fracture load was found to be increasing as travel speed increased from 50 to 100 and slightly decreased at 150 mm/min, as shown in figure 4.15. On the other hand, at 50 mm/min travel speed, fracture load increased as the rotational speed increased from 250 to 500 rpm then decreased at 1000 RPM, as can be seen from figure 4.16. This was attributed to the cracks at the interface and the formation of intermetallic compounds at the interface with different thickness.

The effect of rotational and travel speeds on the clad joint strength were studied, the tensile shear test results of all cladded samples were compared in terms of the maximum fracture load of the joint. The maximum shear load of 4569.452 N was found when a combination of 500 RPM rotational speed and 50 mm/min travel speed were applied to produce the joint (B50), as shown in figure 4.16.

The shear strength of B150 joint was found to be closer to the shear strength of the base aluminum sheet, and failure occurred at the advancing side of the processed zone as shown in figure 4.17. Samples A50 and C50 had failure by slipping at the joint samples without the appearance of necking as in sample A100, B50 and B50 which means the strength of the joint was higher than the yield strength of processed aluminium alloy.

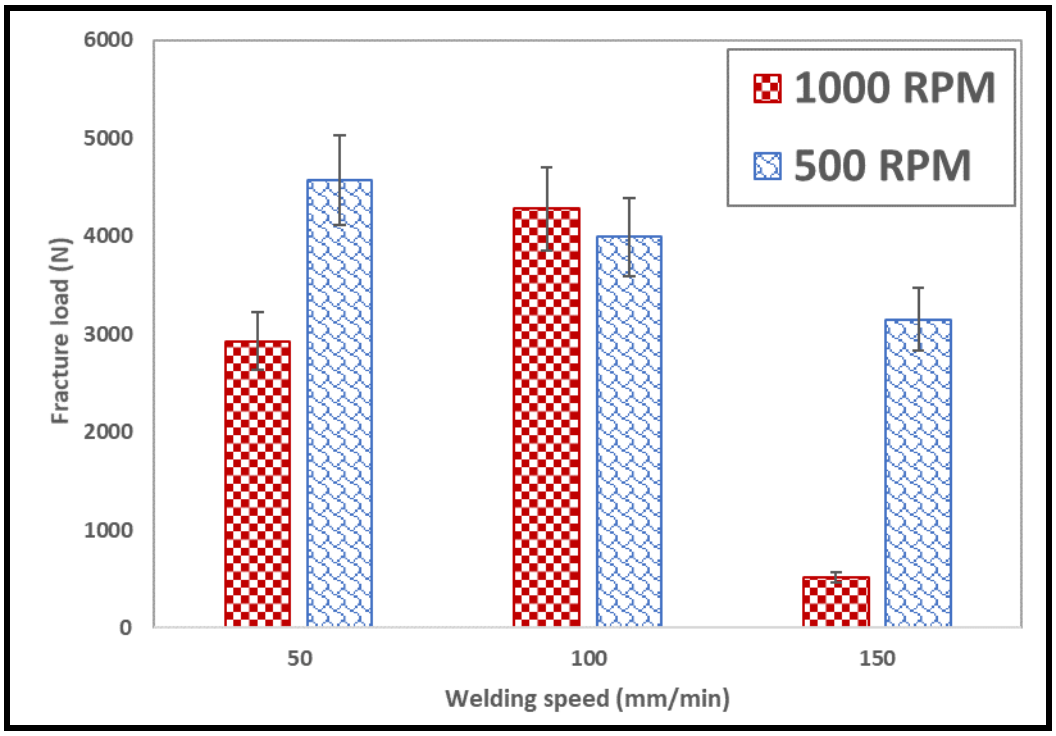


**Figure 4.14:**The effect of traveling speed on the fracture load at rotational speed of 1000 and 500 rpm.

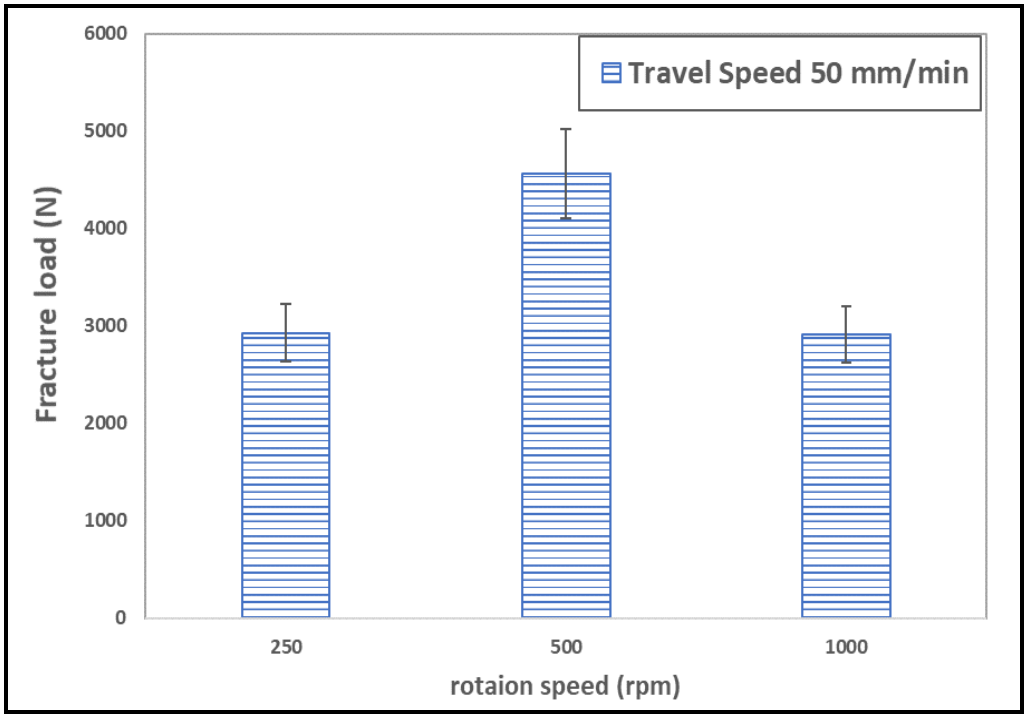


**Figure 4.15:** The effect of rotational speed on the joint fracture load at fixed travel speed of 50 mm/min.

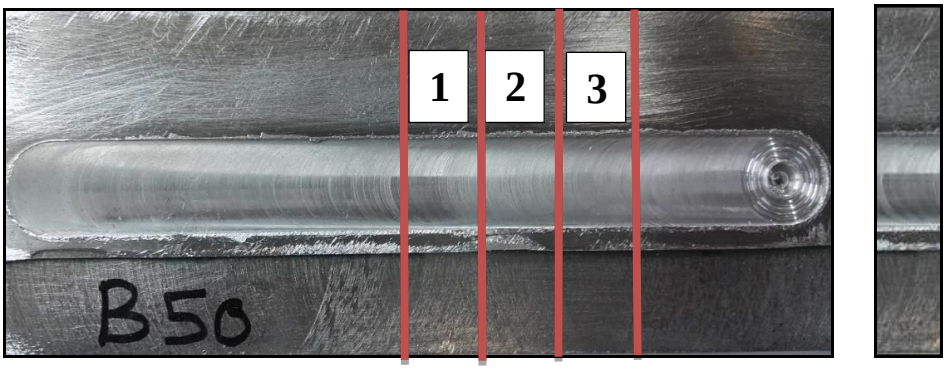


**Figure 4.16:** Tensile shear test specimen

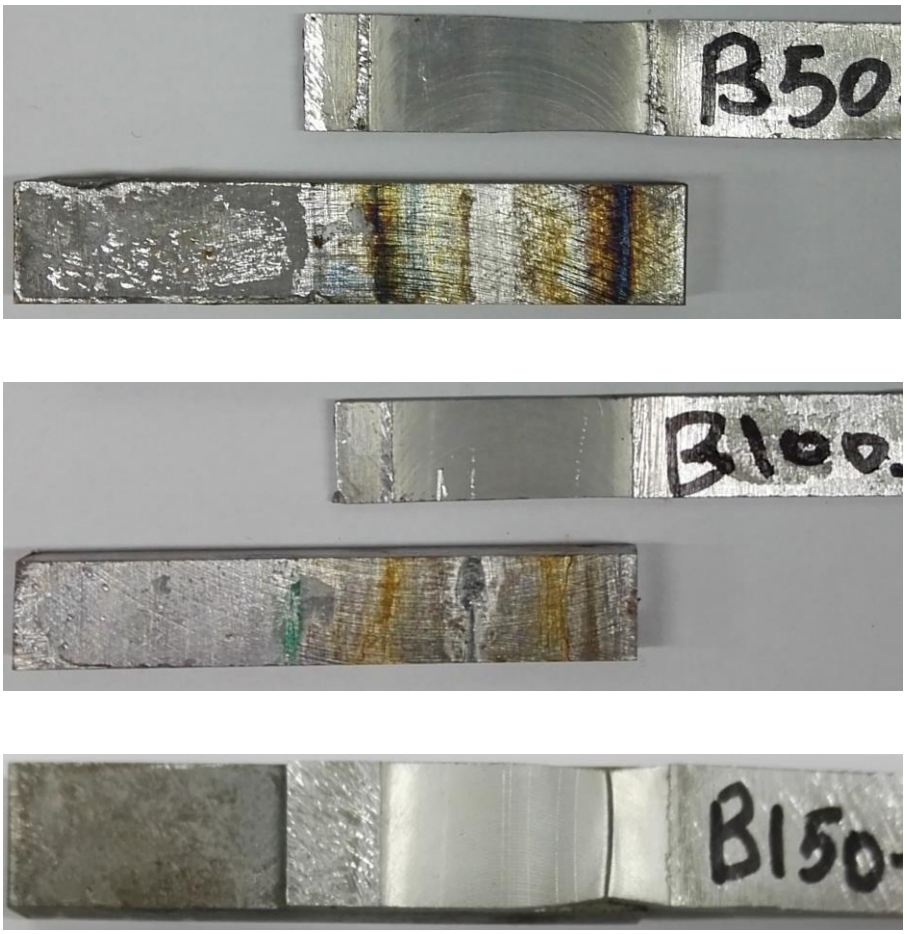


**Figure 4.17:**The tensile shear failure locations at samples B50, B100 and B150

## 4.4 Corrosion (electrochemical test) results

The impedance spectrum of the cladded samples in 3.5% NaCl solution at room temperature were conducted after one hour, one day, one week, two weeks and three weeks of immersion and followed by EIS experiment at open circuit potential, OCP. The Nyquist plots are presented in the Figure 4.18 (a) and (b) respectively. The Nyquist plots shows the behavior of cladded samples with larger values of real and imaginary components.

From figure 4.18 it can be seen clearly that; the cladded system showed better corrosion resistance when compared to Al base metal. According to the Nyquist curves in Figure 4.18, the impedance values can be seen to increase in the order of C50 < A50 < B50, the corrosion resistance trend depends on the heat input; Optimum > intermediate > higher > lowest, heat inputs. However, B50 showed higher impedance values than other samples, because it is defect free and has thicker IMCs layer (4 μm) at the joint interface compared with the other samples**.**

On the other hand, the potentiodynamic polarization experiment for cladded samples has been performed in 3.5% NaCl solution at room temperature after immersion duration of three weeks (504 H) under OCP at a scan rate of 1mV/sec with a frequency range between 100 kHz and 10 mHz. After three weeks of immersion, steady conditions were obtained and then potentiodynamic polarization scan were carried out to investigate the resistivity and stability of the 5052-aluminum alloy clad layer in 3.5 wt. % NaCl solution as shown in figure 4.20.

The polarization parameters of all FSDC samples after 504-hour immersion in 3.5 wt.% NaCl were listed in table 4.6, sample B50 showed higher Ecorr values than that

of the other samples, the passive current density was observed to be similar for all clad samples except for B50 as seen in table 4.6. The cathodic behavior of sample C50 and un-processed aluminum alloy sheet were almost the same, while sample A50 and A100 were similar, unlike sample B50 and B100 as shown in the figure 4.19.

The higher Icorr value of sample B50 was attributed to the thickness of the IMCs at the interface compared to other samples.

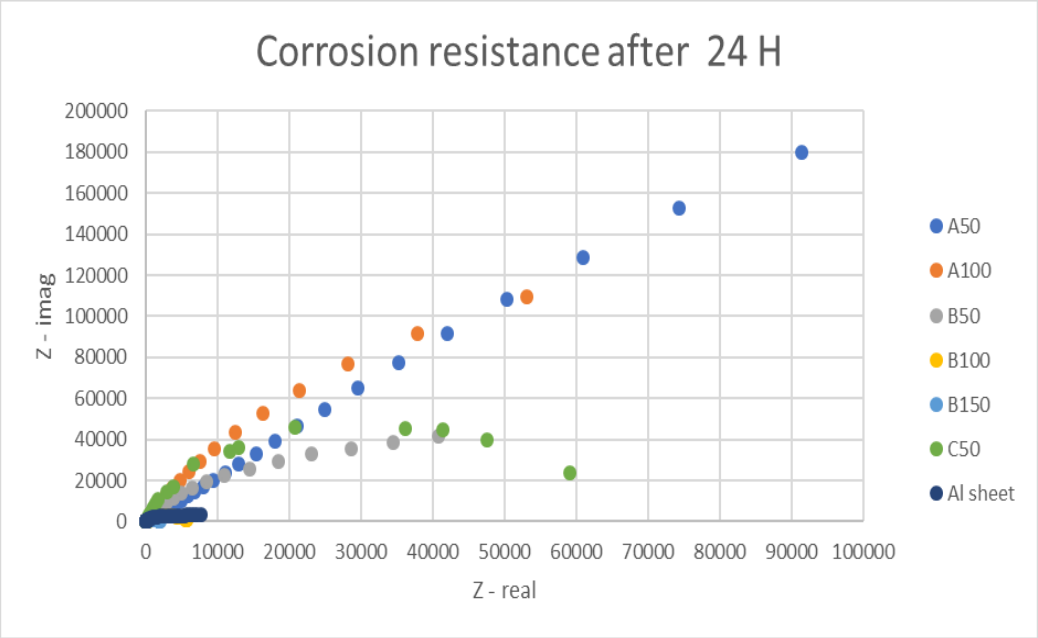


a)

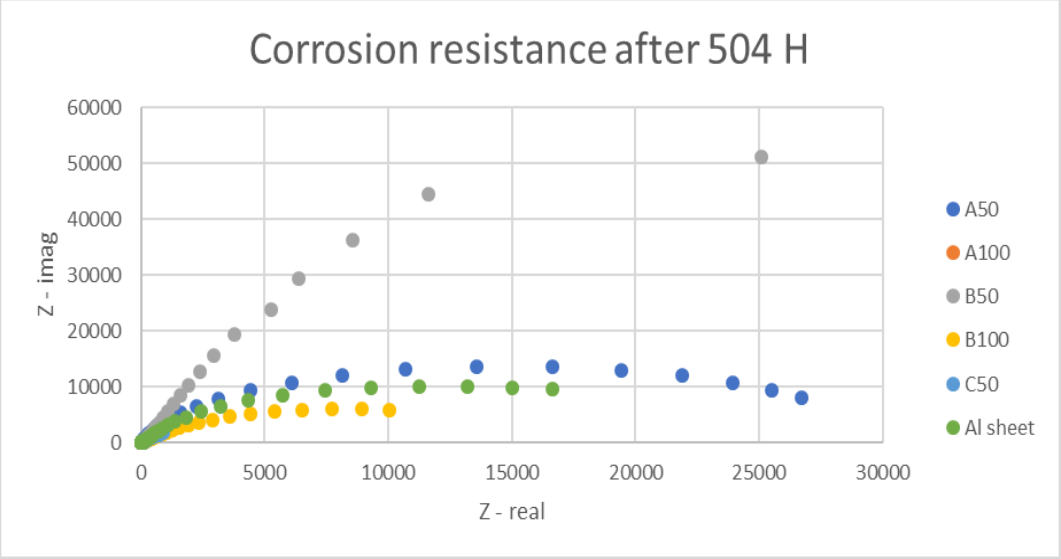


b)

**Figure 4.18:** EIS Nyquist plots after immersion duration of 24 and 504 hours for all cladded samples produced at different FSDC process parameters.

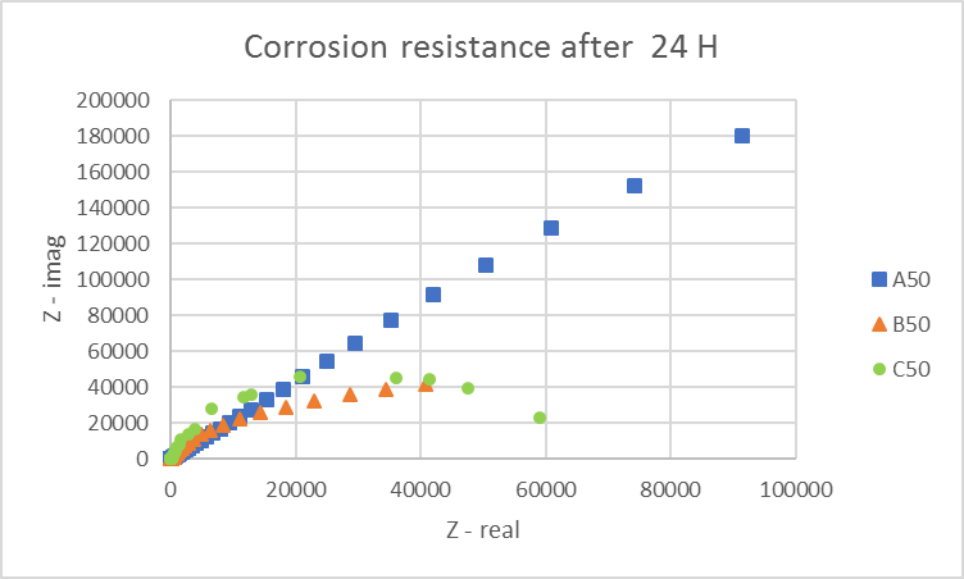


a)

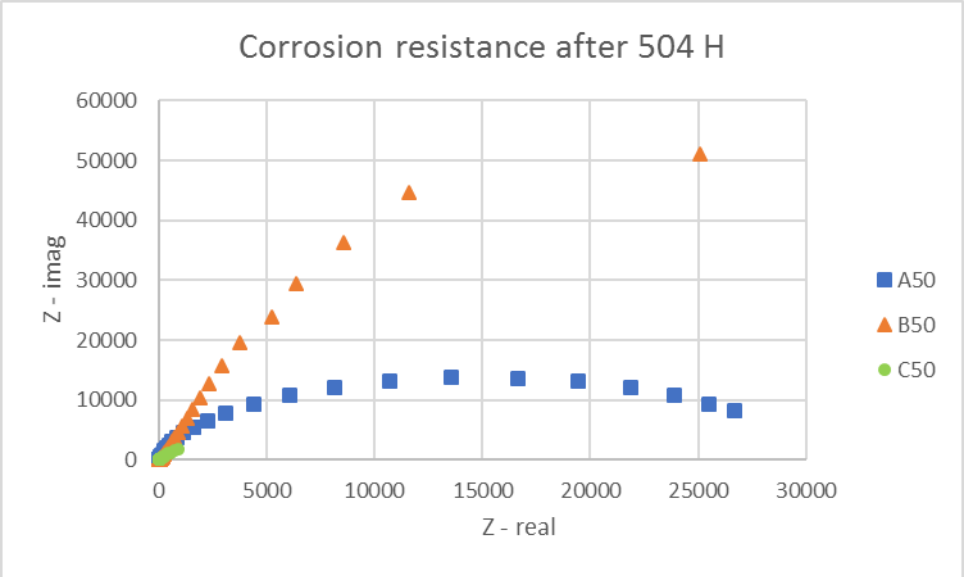


b)

**Figure 4.19:** EIS Nyquist plot for the effect of rotational speeds on corrosion resistance after a) 24 H, b) 504 H

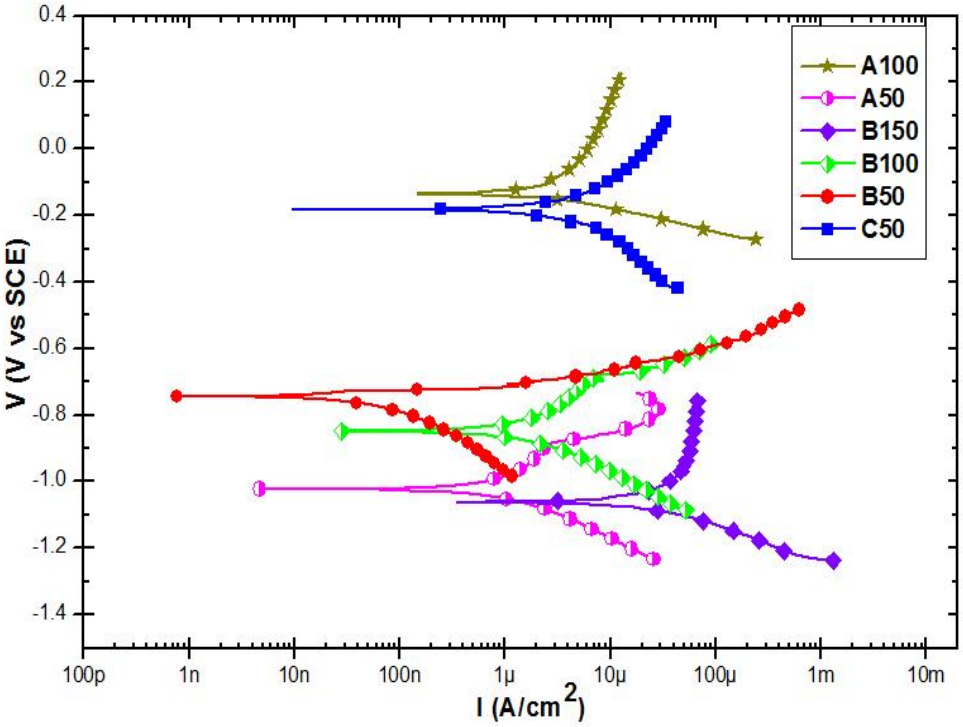


**Figure 4.20: Shows the potentiodynamic polarization curves of all cladded samples at room temperature.**

**Table 4.7: The polarization parameters of all FSDC samples after 504-hour immersion in 3.5 wt.% NaCl.**

| Sample | $E_{corr}$ (mV) | $I_{corr}$ (A $cm^{-2}$) | Beta A (V/decade) | Beta C (V/decade) | Corrosion Rate (mpy) |
|---|---|---|---|---|---|
| **A50** | $-1.02 \times 10^{3}$ | $2.77 \times 10^{-6}$ | 2.041 | $236 \times 10^{-3}$ | 1.265 |
| **A100** | -135 | $2.40 \times 10^{-6}$ | $324.8 \times 10^{-3}$ | $50.40 \times 10^{-3}$ | 1.098 |
| **B50** | -744.0 | $84.00 \times 10^{-9}$ | $188.10 \times 10^{-3}$ | $188.9 \times 10^{-3}$ | $38.39 \times 10^{-3}$ |
| **B100** | -848.0 | $2.750 \times 10^{-6}$ | $397.0 \times 10^{-3}$ | $194.9 \times 10^{-3}$ | 1.259 |
| **C50** | -182.0 | $5.210 \times 10^{-6}$ | $228.5 \times 10^{-3}$ | $202.80 \times 10^{-3}$ | 2.379 |
| **Al -sheet** | -972.0 | $1.14 \times 10^{-6}$ | $321.3 \times 10^{-3}$ | $181.10 \times 10^{-3}$ | $522.9 \times 10^{-3}$ |

# Chapter 5

# Conclusions and Recommendations

In the present work, friction stir diffusion cladding (FSDC) of selected Aluminum grade 5052- H32 to ASTM 516 grade 70 was studied using experimental approach, and process parameters that gave the maximum joint strength and the maximum corrosion resistance had been identified. The effect of FSDC process parameters were studied by considering different rotational and traveling speeds at constant plunging depth and tool tilt angle. The following conclusions can be drawn from this study:

1) FSDC process was developed and ASTM 516-70 steel was successfully cladded with Al 5052-H32 alloys.

2) It is very important to control all the process parameters like; pin depth, rotational and travel speeds, and tool tilt angle in order to reduce the thickness of the intermetallic compounds and enhance the joint quality.

3) A combination of high rotational and high travel speeds result in surface defects such as lack of fill and voids on the surface. Defect free surface was achieved at 500 rpm rotational speed and 50 mm/min welding speed.

4) A combination of low rotational and high travel speeds result in weak bonding at the interface with disbandment of the cladding material.

5) Better mechanical properties were obtained at optimum combination rotational and travel speeds (500 rpm-50 mm/min and 1000 rpm-100 mm/min). The maximum shear load of 4569 N was found when 500 RPM rotational speed and 50 mm/min welding speed were applied to produce the joint (B50).

6) The value of Advance per revolution (APR) has considerable influence on the surface roughness as well as the corrosion resistance. As this ratio increases the surface roughness increases too and vice versa

7) The Hardness at the interface was found higher than that of the substrate material due to the formation of intermetallic phase $Al_{13}Fe_4$ (the maximum value was 429 HV).

8) It was found that as the welding speed increases or decreasing the rotational speed, the grain size closed to the interface decreases due to the low heat input and vice versa.

9) The process parameters that give the best combination of corrosion resistance and joint strength were found to be 500 RPM rotational speed and 50 mm/min welding speed.

This research work represents the bases to break through the friction stir diffusion cladding process of dissimilar metals and alloys, and from the results, we recommend the followings:

1) Expanding the research work of FSDC process to investigate the effect of the other process parameters such as: plunging depth, tool title angle, process direction, tool geometry (shoulder and pin diameters) on the clad quality.
2) Studying the effects of dwell time and plunging rate on joint integrity.
3) Implementation of other corrosion tests to fully understanding the corrosion mechanism such as galvanic corrosion.

# References


[1] N. I. S. Hussein, S. R. Kamarul, and M. N. Ayof, "Preliminary Study of on Cladding Process on Gray Cast Iron Substrate," *Int. J. Res. Eng. Technol.*, vol. 2, no. 11, pp. 5–11, 2013.

[2] V. E. Buchanan, P. H. Shipway, and D. G. McCartney, "Microstructure and abrasive wear behaviour of shielded metal arc welding hardfacings used in the sugarcane industry," *Wear*, vol. 263, no. 1–6 SPEC. ISS., pp. 99–110, 2007.

[3] M. Schneider, "Laser cladding with powder," *Twente (Netherlands), Univ. Dissetation*, 1998.

[4] T. Matsuyama, T. Tsumura, and K. Nakata, "Novel Solid State Cladding of Brass to Steel Plate by Friction Stir Welding *," 2012.

[5] A. A. van der Stelt, T. C. Bor, H. J. M. Geijselaers, R. Akkerman, and A. H. van den Boogaard, "Cladding of Advanced Al Alloys Employing Friction Stir Welding," *Key engineering materials*. 29-May-2013.

[6] K. Komvopoulos and K. Nagarathnam, "Processing and characterization of laser-cladded coating materials," *J. Eng. Mater. Technol.*, vol. 112, no. 2, pp. 131–143, 1990.

[7] S. Liu *et al.*, "Friction Surface Cladding; an exploratory study of a new solid state cladding process," *J. Mater. Process. Technol.*, vol. 229, pp. 769–784, 2016.

[8] J. R. Davis, "Stainless Steel verlays ladding and Weld Hot Roll Bonding," *ASM Spec. Handb.*, 1994.

[9] "httplaserautomation." [Online]. Available: https://goo.gl/images/CDzhGM.

[10] Z. Shen, Y. Chen, M. Haghshenas, T. Nguyen, J. Galloway, and A. P. Gerlich, "Interfacial microstructure and properties of copper clad steel produced using friction stir welding versus gas metal arc welding," *Mater. Charact.*, vol. 104, no. October, pp. 1–9, 2015.

[11] T. N. No, T. T. Note, T. Note, and P. Plain, "CLADDING METALS 1 - Ferrous Metals," no. 22, pp. 1–8, 2000.

[12] R. S. Mishra and Z. Y. Ma, "Friction stir welding and processing," *Mater. Sci. Eng. R Reports*, vol. 50, no. 1–2, pp. 1–78, 2005.

[13] M. Society, "Friction Stir Brazing : a Novel Process for Fabricating Al / Steel Layered Composite and for Dissimilar Joining of Al to Steel," 2011.

[14] H. Bang, H. Bang, G. Jeon, I. Oh, and C. Ro, "Gas tungsten arc welding assisted hybrid friction stir welding of dissimilar materials Al6061-T6 aluminum alloy and STS304 stainless steel," *Mater. Des.*, vol. 37, pp. 48–55, 2012.

[15] Y. C. Chen and K. Nakata, "Effect of the Surface State of Steel on the Microstructure and Mechanical Properties of Dissimilar Metal Lap Joints of Aluminum and Steel by Friction Stir Welding," *Metall. Mater. Trans. A*, vol. 39, no. August 2008, 2008.

[16] R. W. Revie, "Corrosion and corrosion control," 2017. [Online]. Available: https://www.weldingis.com/friction-stir-welding/.

[17] A. Kurt, I. Uygur, and E. Cete, "Journal of Materials Processing Technology Surface modification of aluminium by friction stir processing," *J. Mater. Process. Tech.*, vol. 211, no. 3, pp. 313–317, 2011.

[18] A. Elrefaey, M. Gouda, M. Takahashi, and K. Ikeuchi, “Characterization of Aluminum / Steel Table 1 Chemical composition of the commercially pure,” vol. 14, no. February, pp. 10–17, 2005.
[19] A. Soltani, M. Shakeri, S. Nourouzi, and H. Jamshidi, “Effect of Friction Stir Welding Parameters on Mechanical Properties of Aluminum Alloy to Austenitic Stainless Steel Lap Joint,” *Amirkabir J. Sci. Res. (Mechanical Eng. (AJSR - ME)*, vol. 46, no. 2, pp. 13–15, 2014.
[20] Y. C. Chen and K. Nakata, “Evaluation of microstructure and mechanical properties in friction stir processed SKD61 tool steel,” *Mater. Charact.*, vol. 60, no. 12, pp. 1471–1475, 2009.
[21] K. Kimapong and T. Watanabe, “Lap joint of A5083 aluminum alloy and SS400 steel by friction stir welding,” *Mater. Trans.*, vol. 46, no. 4, pp. 835–841, 2005.
[22] K. Kimapong and T. Watanabe, “Effect of welding process parameters on mechanical property of FSW lap joint between aluminum alloy and steel,” *Mater. Trans.*, vol. 46, no. 10, pp. 2211–2217, 2005.
[23] A. Elrefaey, M. Takahashi, and K. Ikeuchi, “Friction-Stir-Welded Lap Joint of Aluminum to Zinc-Coated Steel,” *Q. J. Japan Weld. Soc.*, vol. 23, no. 2, pp. 186–193, 2005.
[24] Y. C. Chen, T. Komazaki, Y. G. Kim, T. Tsumura, and K. Nakata, “Interface microstructure study of friction stir lap joint of AC4C cast aluminum alloy and zinc-coated steel,” *Mater. Chem. Phys.*, vol. 111, no. 2, pp. 375–380, 2008.
[25] K. Kimapong and T. Watanabe, “Effect of welding process parameters on mechanicl properties of {FSW} lap joint between aluminium alloy and steel,” *Mater. Trans.*, vol. 46, no. 2211–2217, pp. 2211–2217, 2005.
[26] Z. W. Chen and S. Yazdanian, “Friction Stir Lap Welding : material flow , joint structure and strength,” *J. Achiev. Mater. Manuf. Eng.*, vol. 55, no. 2, pp. 629–637, 2012.
[27] P. R. Kalvala, J. Akram, and M. Misra, “Friction assisted solid state lap seam welding and additive manufacturing method,” *Def. Technol.*, vol. 12, no. 1, pp. 1–9, 2015.
[28] Y. Zhao, Z. Ding, C. Shen, and Y. Chen, “Interfacial microstructure and properties of aluminum-magnesium AZ31B multi-pass friction stir processed composite plate,” *Mater. Des.*, vol. 94, pp. 240–252, 2016.
[29] K. Kimapong and T. Watanabe, “Effect of Welding Process Parameters on Mechanical Property of FSW Lap Joint between Aluminum Alloy and Steel,” *Mater. Trans.*, vol. 46, no. 10, pp. 2211–2217, 2005.
[30] Y. Gao, K. Nakata, K. Nagatsuka, T. Matsuyama, Y. Shibata, and M. Amano, “Microstructures and mechanical properties of friction stir welded brass/steel dissimilar lap joints at various welding speeds,” *Mater. Des.*, vol. 90, pp. 1018–1025, 2016.
[31] T. Saeid, A. Abdollah-zadeh, and B. Sazgari, “Weldability and mechanical properties of dissimilar aluminum-copper lap joints made by friction stir welding,” *J. Alloys Compd.*, vol. 490, no. 1–2, pp. 652–655, 2010.
[32] S. R. Sharma, Z. Y. Ma, and R. S. Mishra, “Effect of friction stir processing on fatigue behavior of A356 alloy,” vol. 51, pp. 237–241, 2004.
[33] M. L. Santella, “Effects of friction stir processing on mechanical properties of the

cast aluminum alloys A319 and A356 q," vol. 53, pp. 201–206, 2005.
[34] S. Dodds, A. H. Jones, and S. Cater, "Tribological enhancement of AISI 420 martensitic stainless steel through friction-stir processing," *Wear*, vol. 302, no. 1–2, pp. 863–877, 2013.
[35] H. S. Grewal, H. S. Arora, H. Singh, and A. Agrawal, "Applied Surface Science Surface modification of hydroturbine steel using friction stir processing," *Appl. Surf. Sci.*, vol. 268, pp. 547–555, 2013.
[36] K. P. Rao, G. D. J. Ram, and B. E. Stucker, "Effect of friction stir processing on corrosion resistance of aluminum – copper alloy gas tungsten arc welds," *Mater. Des.*, vol. 31, no. 3, pp. 1576–1580, 2010.
[37] H. K. Rafi, G. D. J. Ram, G. Phanikumar, and K. P. Rao, "Microstructural evolution during friction surfacing of tool steel H13," *Mater. Des.*, vol. 32, no. 1, pp. 82–87, 2011.
[38] J. P. Bergmann, F. Petzoldt, R. Schürer, and S. Schneider, "Solid-state welding of aluminum to copper - Case studies," *Weld. World*, vol. 57, no. 4, pp. 541–550, 2013.
[39] A. Roos, J. F. dos Santos, T. Donath, J. Herzen, and F. Beckmann, "Validation of Diffusion Processes by muCT of Marker Material in new Friction based Hybrid Friction Diffusion Bonding (HFDB) Process," *HASYLAB Annu. Rep.*, pp. 775–776, 2006.
[40] A. Forcellese, F. Gabrielli, and M. Simoncini, "Mechanical properties and microstructure of joints in AZ31 thin sheets obtained by friction stir welding using 'pin' and 'pinless' tool configurations," *Mater. Des.*, vol. 34, pp. 219–229, 2012.
[41] Z. Hongwei, Z. Xuehua, and Z. Bao'an, "System Dynamics Approach to Urban Water Demand Forecasting," *Trans. Tianjin Univ.*, vol. 15, no. 1, pp. 70–74, 2009.
[42] D. Bakavos, Y. Chen, L. Babout, and P. Prangnell, "Material interactions in a novel pinless tool approach to friction stir spot welding thin aluminum sheet," *Metall. Mater. Trans. A Phys. Metall. Mater. Sci.*, vol. 42, no. 5, pp. 1266–1282, 2011.
[43] A. J. Davenport, M. Jariyaboon, C. Padovani, N. Tareelap, B. J. Connolly, and S. Williams, "Corrosion and Protection of Friction Stir Welds," vol. 521, pp. 699–704, 2006.
[44] M. Jariyaboon, A. J. Davenport, R. Ambat, B. J. Connolly, S. W. Williams, and D. A. Price, "The effect of welding parameters on the corrosion behaviour of friction stir welded AA2024-T351," *Corros. Sci.*, vol. 49, no. 2, pp. 877–909, 2007.
[45] K. Surekha, B. S. Murty, and K. P. Rao, "Microstructural characterization and corrosion behavior of multipass friction stir processed AA2219 aluminium alloy," *Surf. Coatings Technol.*, vol. 202, no. 17, pp. 4057–4068, 2008.
[46] K. Surekha, B. S. Murty, and K. Prasad Rao, "Effect of processing parameters on the corrosion behaviour of friction stir processed AA 2219 aluminum alloy," *Solid State Sci.*, vol. 11, no. 4, pp. 907–917, 2009.
[47] W. Xu and J. Liu, "Microstructure and pitting corrosion of friction stir welded joints in 2219-O aluminum alloy thick plate," *Corros. Sci.*, vol. 51, no. 11, pp. 2743–2751, 2009.
[48] R. Grilli, M. A. Baker, J. E. Castle, B. Dunn, and J. F. Watts, "Localized corrosion of a 2219 aluminium alloy exposed to a 3.5% NaCl solution," *Corros. Sci.*, vol. 52,

no. 9, pp. 2855–2866, 2010.
[49] K. Surekha, B. S. Murty, and K. Prasad Rao, “Comparison of corrosion behaviour of friction stir processed and laser melted AA 2219 aluminium alloy,” *Mater. Des.*, vol. 32, no. 8–9, pp. 4502–4508, 2011.
[50] H. long Qin, H. Zhang, D. tong Sun, and Q. yu Zhuang, “Corrosion behavior of the friction-stir-welded joints of 2A14-T6 aluminum alloy,” *Int. J. Miner. Metall. Mater.*, vol. 22, no. 6, pp. 627–638, 2015.
[51] M. Jariyaboon, a. J. Davenport, R. Ambat, B. J. Connolly, S. W. Williams, and D. a. Price, “Corrosion of a dissimilar friction stir weld joining aluminium alloys AA2024 and AA7010,” *Corros. Eng. Sci. Technol.*, vol. 41, no. 2, pp. 135–142, 2006.
[52] B. Brown, “Corrosion Resistance of Aluminum CRANE MATERIALS INTERNATIONAL A Whitepaper by :,” *System*, pp. 1–6, 2011.
[53] C. G. Padovani *et al.*, “Corrosion and Protection of Friction Stir Welds in Aerospace Aluminium Alloys,” *La Metall. Ital.*, pp. 29–42, 2008.
[54] A. . Zuruzi, H. Li, and G. Dong, “Effects of surface roughness on the diffusion bonding of Al alloy 6061 in air,” *Mater. Sci. Eng. A*, vol. 270, no. 2, pp. 244–248, 1999.
[55] “Mechanical and Physical properties of Al 5052 and ASTM A516-70 steel.” [Online]. Available: http://www.matweb.com/search/datasheet.aspx?matguid=9ccee2d0841a404ca504620085056e14&ckck=1.
[56] Y. N. Zhang, X. Cao, S. Larose, and P. Wanjara, “Review of tools for friction stir welding and processing,” *Can. Metall. Q.*, vol. 51, no. 3, pp. 250–261, Jul. 2012.
[57] W. B. Lee, Y. M. Yeon, and S. B. Jung, “Joint properties of friction stir welded AZ31B– H24 magnesium alloy,” *Mater. Sci. Technol.*, vol. 19, no. 6, pp. 785–790, 2003.
[58] C. G. Rhodes, M. W. Mahoney, W. H. Bingel, and M. Calabrese, “Fine-grain evolution in friction-stir processed 7050 aluminum,” *Scr. Mater.*, vol. 48, no. 10, pp. 1451–1455, 2003.

# Vitae


Name : Almigdad Babiker Hamid Ibrahim

Nationality : Sudanese

Date of Birth :11/9/1988

Email : almigdadbabiker@gmail.com

Address : Khartoum, Sudan


Academic Background :

MSc. (Mechanical Engineering), May 2017

King Fahd University of Petroleum and Minerals Dhahran, Kingdom of Saudi Arabia.

BSc. (Mechanical Engineering), October 2012

University of Khartoum

Khartoum, Sudan.

Research Interests :

Joining similar and dissimilar materials, Additive /Rapid manufacturing, Subtractive manufacturing, Surface engineering, Wear of materials and Composite materials.

Publications :

**Almigdad Babiker**, Fadi Al-Badour, Rami Suleiman, Ahmad Sorour, Friction Stir Diffusion Cladding of Aluminum Alloy on Cold Rolled Carbon Steel, Advance Computational Engineering and Experimenting (ACE-X), July 2017 (accepted manuscript).

**Almigdad B. Ibrahim**, Rami Suleiman, Akeem Y. Adesina, Fadi A. Al-Badour, Corrosion Behavior of Friction Stir Diffusion Cladded ASTM A 516-70 Steel With 5052 Aluminum Alloy, *Materials Performance and Welding Technologies Conference (MPWT-17)*, Sept. 2017, (accepted manuscript).

Akeem Yusuf Adesina, Fadi A. Al-Badour, **Almigdad B. Ibrahim**, Zuhair M. Gasem, Electrochemical Analysis of Friction Stir Welded 304 Stainless Steel in Acidic Medium,

Materials Performance and Welding Technologies Conference (MPWT-17), Sept. 2017, (accepted manuscript).